

# รายงานวิจัยฉบับสมบูรณ์

โครงการศึกษาการม้วนพับตัวและเสถียรภาพของโปรตีนสารพิษจาก *Bacillus thuringiensis* Folding and Stability Analysis of Insecticidal Proteins from *Bacillus thuringiensis* 

โดย นายชาติชาย กฤตนัย

กรกฎาคม 2547

# รายงานวิจัยฉบับสมบูรณ์

โครงการศึกษาการม้วนพับตัวและเสถียรภาพของโปรตีนสารพิษจาก *Bacillus thuringiensis* Folding and Stability Analysis of Insecticidal Proteins from *Bacillus thuringiensis* 

ผู้วิจัย

นายชาติชาย กฤตนัย สถาบันอณูชีววิทยาและพันธุศาสตร์ มหาวิทยาลัยมหิดล

สนับสนุนโดยสำนักงานกองทุนสนับสนุนการวิจัย

# สารบัญ

กิตติกรรมประกาศ	1
บทคัดย่อภาษาอังกฤษ	2
บทคัดย่อภาษาไทย	3
เนื้อหางานวิจัย	
Introduction	5
Materials and Methods	11
Results and Discussions	17
Concluding Remarks	
References	53
Outputs ที่ได้รับจากการวิจัย	60
ภาคผนวก / ผลงานตีพิมพ์	

เนื้อหาสรุปของงานวิจัย

#### INTRODUCTION

### The Protein Folding Problem

Based upon an extensive characterization of the genomes in several organisms, a vast numbers of proteins have been identified and explored. The major question that always came up with the functional proteins is how proteins fold from the amino acid sequence in primary structure to a unique tertiary structure. There are several reasons contributed for the investigation of protein folding problem, including (i) to understanding the mechanism underlying protein misfolding or aggregation in several human diseases, such as prion-, Huntingtion's- and Alzheimer's diseases (1-3). (ii) to develope effective strategies for ensuring that recombinant polypeptides fold to their native structure in industrial and research applications. (iii) to investigate enzymatic activity under severe conditions, such as in organic co-solvent solutions, is seen as a potentially new method for chemical synthesis (4, 5).

According to Levinthal's paradox, (6) it is impossible that the amino acid sequence in unfolded protein is randomly folded, searching for the native one. The protein must have the specific pathway to fold in compatible with biological processes. Anfinsen's dogma (7-9) derived from the spontaneous refolding of ribonuclease A after denaturation, also revealed that the destination map of protein folding was embedded within the amino acid sequence itself. Nowadays, the further understanding of the protein folding problem is greatly assisted by a numbers of methods of high structural and kinetic resolution in the time scale ranging from microseconds to seconds (10-15) and highly resolved X-ray structure of proteins.

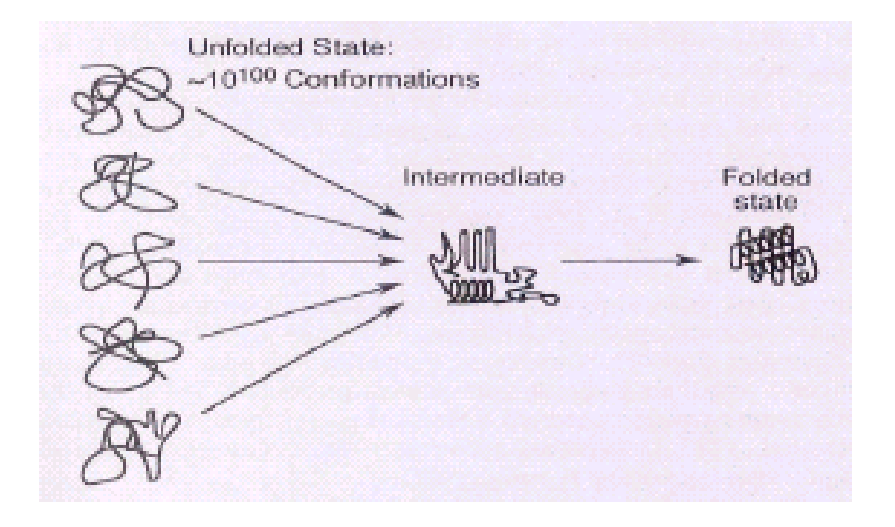


**Figure 1:** Protein Folding Paradox: The proteins fold in seconds or faster. What makes the folding so rapid compared to a random walk? What is the mechanism that has involved? What are the pathways of folding? (16)

Basic concept on the analysis of conserved residues in evolutionary and functionally related proteins whose sequences have been diverged in evolution reveals two types of conserved residues. Conserved residues in the functionally part are usually located in active site, while another do not involve with the function and therefore could be related to folding of protein (17).

Many investigations have revealed that the identity of residues participating in the rate-limiting step of folding might be conserved. If evolution acts at the level of fine sequence details in order to produce and maintain rapid folding, conservation of residue identity and structures might be expected within families of homologous proteins or across protein superfamilies including those of CI-2, cytochrome c, ubiquitin, CheY, ADAh2 and CD2 (18-22). One of the examples is the large family of c-type cytochromes. It is one of the oldest protein families since this protein serves for utilization of the external energy, which is the main feature of life. The c-type cytochromes have about 1.5 billion years of evolution and their sequences have diverged so much. The chain lengths of these proteins vary from about 60 to more than 200. Despite these very large differences in sequences, the 3D structures of all the c-type cytochromes are similar (17). These suggested that the interactions of the conserved region might play the significant role to maintain their molecular folding.

#### Stabilizing Interactions of Protein Structure

There are many interactions and forces that can stabilize the folding of protein. The major ones can be classified to include van der Waals forces, hydrophobic interaction, hydrogen bonding and electrostatic interactions. Van der Waals forces can be distinguished into attractive and repulsive forces. These forces are formed between induced dipole atoms rising from fluctuations in the electron charge densities of neighboring non-bonded atom. If two molecules are held together exclusively by van der Waals forces, their average seperation is governed by a balance between the van der Waals attractive and repulsive forces. This force is normally considered as a weak, short ranged and non-specific interaction.

Hydrophobic interaction is found among the hydrophobic residues of protein. It involves with the entropic factor. Because these interactions between side chain of amino acids are more favorable in the water-less environment, hydrophobic amino acid tend to be located at the protein interior (23, 24). Even though one believes that the hydrophobic interaction is the first driving force of protein folds, other interactions are still contributing in maintaining and stabilizing of the folded structure.

Hydrogen bonds is defined as a partial sharing of a hydrogen atom between two electronegative atoms. There are a large number of H-bond donor and H-bond acceptor located on the side chain and also in secondary structure backbone known as alpha helix and beta sheet. The Gibbs energy contributions per hydrogen bond in the interior of protein are estimated to be around 2-10 kcal/mol. It has been previously reported that H-bonds between side chain of amino acid residues also play a significant role in the transitional state during protein folding (25).

Electrostatic interaction can be categorized into repulsive and attractive interactions. The strength of this interaction depends on interacted charges, dielectric constant and the distance between them. The strengths of these interactions are vary significantly depends upon their location within the protein structure. In the case of interaction inside protein interior in which its dielectric constant is much lower than exterior, the strength of electrostatic interaction is much more significant. The orientation of the salt bridging side chain with respect to one another is also the factor of the strength of the interaction. An interacting energy between a pair of charged residues are directly correlated with the pKa values of the individual charged residues. This interaction has been reported to play an important role in protein structure and function such as oligomerization, molecular recognition and cooperativity in protein folding (26-28).

#### **Protein Unfolding and Stability**

Factors affecting molecular stability of protein are temperature, pH, salt concentration and denaturant counterparts (29-42). The most widely used denaturant to investigate protein stability are urea and guanidine hydrochloride (GuHCI). Thermodynamic study of protein unfolding and stability is generally obtained by investigation of the protein from ordered native state (N) to disordered unfolded state (U). In these experiments the native protein will gradually be denatured as the incubating concentrations of denaturant is increased. Conformational changes between native and unfolded state can be monitored by methods such as microcalorimetry and spectroscopy (29-38). In spectroscopic technique, the method of choices are circular dichroism which observes changes of protein secondary structure and intrinsic fluorescence which monitors changes of the tertiary structure packing of protein. These unfolding experiments give an unfolding curve showing conformational changes from native to unfolded state under various concentration of denaturant. An analysis of this curve generally reports a transitional mid-point which is the molarity of denaturant that unfold half

of protein. Further analysis by model fitting can also give specific unfolding free energy (delta G) used in the transition from native to unfolded states (42).

Recently an effort to develop a database for the transitional free energy of protein has established. This database, Protherm (<a href="www.rtc.riken.go.jp/jouhou/Protherm/protherm.html">www.rtc.riken.go.jp/jouhou/Protherm/protherm.html</a>) is a depository of the thermodynamic parameters of proteins and mutants. The entry also includes the different of free energy between wild type and mutants (single, double mutation) under the given conditions. A systematic comparison and analysis of these mutant has led us to examine a contribution of single amino acid residue toward protein folding and stability.

## Bacillus thuringiensis (Bt)

Bacillus thuringiensis is a rod-shaped, gram-positive, spore-forming bacterium that forms a parasporal crystal during the stationary phase of its growth cycle. It was initially characterized as a microbial control agent. The susceptible insects include lepidopteran, dipteran and coleopteran class (43, 44). Since, the larval stage in an insect life cycle is the stage during which most of the feeding occurs, Bt is an effective insecticide for the larvae stage only (http://www.ag.usask.ca/cofa/departments/hort/hortinfo/pests/bt.html). There are several subspecies of Bt, The most common known are subsp. israelensis (Bti) which is toxic to mosquito and blackfly larvae, kurstaki (Btk) and morisoni killing moth and butterfly caterpillars, aizawai killing wax moth caterpillars and tenebrionis killing beetle larvae (http://www.biotech-info.net/Bt\_primer.html.). Other strain of Bt have also been discovered with pesticidal activity against nematodes, mites, flatworms and protozoa (45, 46).

#### **Cry Toxins and General Structures**

The toxic crystal protein produced from *Bacillus thuringiensis* can be named as Cry toxin. The structure of these Cry toxins are composed of 3 domains. Domain I is a bundle of 7 alpha helices. Some of these helices can insert into the gut cell membrane, creating a pore through which ions can pass freely (47-51). Domain II consists of three antiparallel betasheets, similar to the antigen-binding regions of immunoglobulins, suggesting that this domain binds to the receptors or docking protein on the insect gut membrane (52-61). Domain III is a tightly packed beta-sandwich which is suggested to protect the exposed end (C-terminus) of the active toxin and prevent further cleavage by insect gut proteases (62-65).

## **Mechanism of Action of Cry toxins**

As Cry toxins are produced as insoluble 130-kDa protoxins, solubilization and proteolytically processing by proteases are required in an alkali condition within the mid-gut of insect larvae. The resulting 65-kDa active toxins has been proposed to bind with specific protein on mid gut membrane. The killing activity is initiated by a partial insertion of domain I into the cell membrane, an oligomerization to form ion pore. This pore-forming activity can lead to lethal imbalance of ion between inner and outer cell membrane (66-68). The initial binding step of active toxin is suggested to be involved with domain II. Since domain II has the most divergent in sequence among the Cry toxins, it has been described as the specificity-determining domain. A supporting evident is a report that investigated a reciprocal hybrid gene between closely related toxins (Cry1Aa and Cry1Ac) which is resulted in altered specificity (69).

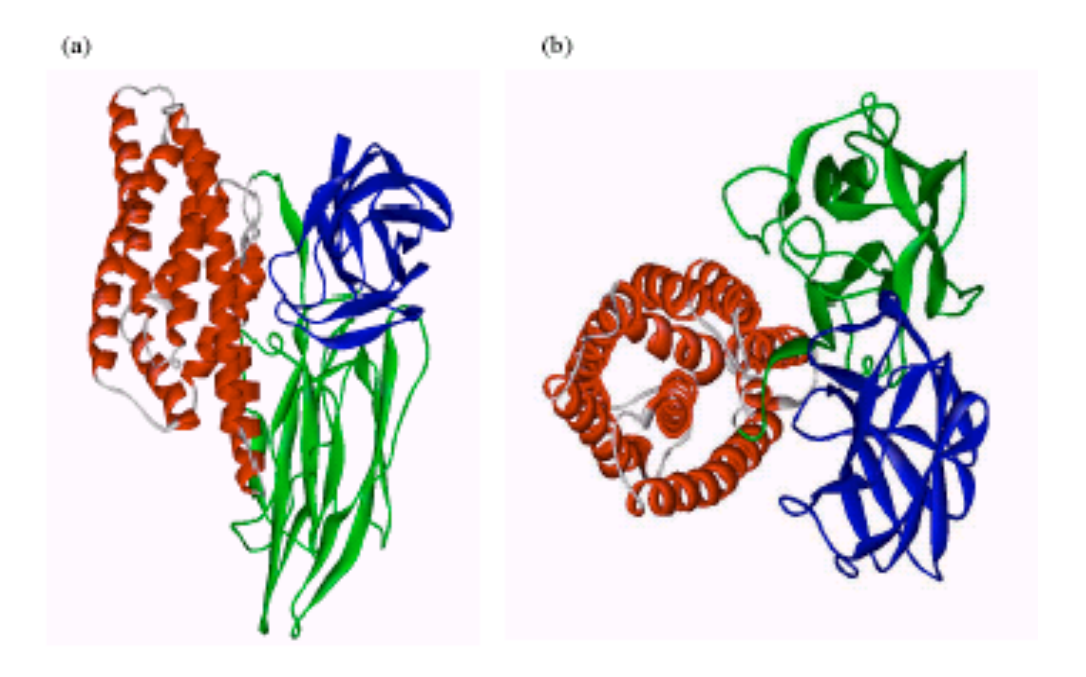


**Figure 2:** Three dimensional structure of Cry3A Toxin (70) showing 3 functional domains in side (a) and top (b) views.

# **Conserved Sequence Blocks Cry Toxins**

According to an alignment of amino acid sequences among the Cry toxins, there are 5 conserved blocks identified in various locations of the general structure (71).

Conserved block 1 is found on the region of helix alpha 5 of domain I. This helix has been proposed to be involved in membrane insertion and pore formation. This significant role

in biological activity might explain its highly conserved nature. This helix 5 has also been suggested to play an essential role in maintaining structural integrity of the helical bundle within the domain I.

Conserved block 2 includes helix alpha 7 on domain I and the first beta-strand on domain II. These two structures comprise the region of contact interface between the two domains. There are three structurally equivalent salt bridges present between domain I and domain II of Cry1Aa and Cry3A. The residues involved lie within block 2. These interaction could be important if domain I changes its orientation relative to the rest of the molecule upon binding of the toxin to its receptor. Alternatively, these salt bridges could be responsible for maintaining the protein in globular form during solubilisation and activation.

Conserved block 3 is located in the interdomain between domain II and domain III. It contains the last beta strand of domain II and the beginning of domain III.

Conserved block 4 and 5 are located side-by-side in domain III. The central two arginines of block 4 may be involved in intermolecular salt bridges affecting crystal or oligomeric aggregation (44).

These 5 conserved blocks are believed to be contributed in the folding and stability of Cry toxins (65, 70-72). Therefore, interactions of the conserved residues within these conserved blocks are examined for their role in stability and folding in this research project.

#### Cry4B Toxin

Cry4B toxin is the crystal protein produced in *Bacillus thuringiensis* subsp. *israelensis* with specific to *Aedes aegypti* mosquito larvae. It is initially produced in 130-kDa protoxin and digested in the alkaline midgut environment to 65-kDa active toxin. The 65-kDa active toxin is further cleaved at the position R-203 to 47-48 kDa and 16-18 kDa fragments (73, 74). To investigate the protein folding, the candidate protein must be the intact fragment, therefore, the mutant, R203Q, was generated to eliminate the internal cleavage of 65-kDa active toxin. General properties of the R203Q mutant such as toxicity, solubility, secondary and tertiary structure profile, is found similar to those of wild type (75).

#### **MATERIALS AND METHODS**

#### 1. Construction of Mutant Plasmid

#### 1.1 Plasmid DNA Extraction

An extraction of DNA from  $E.\ coli$  cell culture is based on the method using cationic detergent cetyl-trimethylammonium bromide (CTAB) for DNA precipitation (79). In general, the E.coli cell was cultured in LB-broth for over night. Cells are collected by centrifugation and re-suspended in STET buffer. The reaction included digestion with lysozyme, ribonuclease A and recovered in 5% CTAB. Extraction was employed by chloroform and precipitated in absolute ethanol at  $-20^{\circ}$ C. DNA pellet was obtained by centrifugation, washed with 70% ethanol and then dried in room temperature.

#### 1.2 DNA Analysis by Agarose Gel Electrophoresis

The gel was prepared in TBE buffer (0.09 M Tris-HCl, 0.09 M Boric acid, 2 mM EDTA pH 8.0), and melted until reaching homogeneity in microwave oven. The gel solution was poured into an electrophoretic tray and allowed to solidify. The TBE buffer was used as an electrophoretic buffer. DNA sample was mixed with gel-loading dye (15% (w/v) Ficoll 400, 0.01% (w/v) Bromophenol blue) and then loaded into the well. After running with appropriate voltage, the gel was stained in ethidium bromide solution and destained in distilled water. The DNA patterns were visualized under UV light and photographed.

## 1.3 Site-Directed Mutagenesis

Site-directed mutagenesis based on the method of Stratagene's QuickChange was employed. The recombinant plasmid with targeted gene, was mutated using complementary oligonucleotide primers containing the desired mutation in the polymerase chain reaction (PCR). The high fidelity polymerase, *Pfu* DNA polymerase, was used in temperature cycling. The mutagenic primers were designed and synthesized based on the selected amino acid. The sample reaction (50 μl) was comprised of 100 ng DNA template, 50 μM for each dNTP, 10 pmole for each forward and reverse primers, 5 μl 10X *pfu* buffer, 2.5 U *Pfu* polymerase, and distilled water to make it to 50 μl. The PCR cycling was set to 95°C 1 min 1 cycle, 95°C 1 min, 44-50°C 1.30 min, 68°C 13 min 18 cycle, and 68°C 7 min 1 cycle. Following temperature cycling, the reaction was added with *Dpn* I, and incubated at 37oC for 3 hours to digest the template DNA.

## 1.4 Preparation of Competent Cells by CaCl, Method

A single colony of *E. coli* strain JM109 was inoculated in 3 ml of LB broth and cultured at  $37^{\circ}$ C with 250 RPM shaking overnight. The starter was diluted 1:100 in 200 ml LB broth and incubated further at  $37^{\circ}$ C and shaking for approximately 2-3 hours until the OD<sub>600</sub> reached 0.3-0.4. The culture was divided into 6 tubes of 50 ml centrifuge tube and placed on ice for 10 minutes. Cells were collected by centrifugation at 4,000 rpm,10 minutes,  $4^{\circ}$ C. The pellet was re-suspended in 20 ml of chilled 0.1 M CaCl<sub>2</sub> and placed on ice 10 minutes before spinning 4,000 rpm for 10 minutes at  $4^{\circ}$ C. The pellet was again resuspended in 4 ml of chilled 0.1 M CaCl<sub>2</sub> for each 200 ml of original culture and placed on ice 15 minutes. The cell was aliquot 100-200  $\mu$ l and kept in 30% (v/v) glycerol at  $-80^{\circ}$ C.

## 1.5 Transformation of Plasmid DNA into Competent Cells

The *Dpn*I-treated PCR product approximately 20-40 ng was added into 200  $\mu$ I competent cells and gently mixed. The transformation reaction was chilled on ice for 30 minutes, then placed in 42°C for exactly 90 seconds and immediately chilled on ice 2-5 minutes. The reaction was added with LB broth 800  $\mu$ I and incubated at 37°C for 1 hour with shaking. The transformed cells were collected by centrifugation at 5,000 rpm for 2 minutes and re-suspended in 200  $\mu$ I of media. The transformation culture was plated on LB agar plate containing 100  $\mu$ g/mI of ampicillin and incubated at 37°C for 16-20 hours.

## 1.6 Restriction Endonuclease Analysis

The analysis was used to screen for the mutant plasmids based on their recognition sites which were introduced by the mutagenic primers. The 20  $\mu$ l of reaction solution contained 100-200 ng of DNA plasmid, 1X restriction enzyme digestion buffer, 1-2 units of restriction enzyme and sterile distilled water to achieve the final volume 20  $\mu$ l. The reaction solution was incubated at optimum temperature for each enzyme for 2-3 hours. The DNA product was analyzed in 0.8-1% agarose gel electrophoresis.

## 1.7 Automated DNA Sequencing Analysis

The DNA sequence of mutant plasmids were confirmed by this analysis using ABI PRISMTM Sequencing Kit. The sequencing reaction was performed on ABI PRISMTM 377 automated DNA sequencer. The principle of this analysis is based on a fluorescent-labeled terminator cycle sequencing (81, 82). The 20 µl of sequencing reaction contained mixture 4 µl of terminator premix (dATP, dCTP, dGTP, dTTP, A-dye terminator, C-dye terminator, G-

dye terminator, T-dye terminator, MgCl<sub>2</sub>, Tris-HCl pH 9.0, thermal stable pyrophosphatase and Amplitaq DNA polymerase), plasmid 300-500 ng of DNA template, 1X sequencing buffer and 10 pmole of oligonucleotide primer. The reaction was placed on an automated thermal cycler with the following condition: 96°C 3 min 1 cycle, 96°C 10 sec, 60°C 4 min 20 cycles, 60°C 7 min 1 cycle. When the PCR reaction was completed, the PCR product was precipitated with 1/10 v/v of 3 M Sodium acetate pH 4.8 and 50 µl of 95% ethanol. The mixture was incubated for 15 minutes at room temperature and centrifuged at 12,000 rpm for 15 minutes. The DNA pellet was then washed with 200 µl of 70% ethanol, dried at room temperature and then analyzed on the ABI PRISMTM 377 automated DNA sequencer.

## 2. Toxin Expression and Purification

# 2.1. Expression of Toxins

E. coli colony was inoculated in 3 ml LB broth containing 100 mg/ml ampicillin and incubated at 37°C 250 rpm for overnight. The overnight culture was transferred into a new flask of LB-ampicillin broth to make up 1% of final concentration. The culture was incubated at 37°C 250 rpm for 2-3 hours until OD600 reached 0.3-0.5. An expression was induced by adding isopropyl-B-D-thiogalactopyranoside (IPTG) with a final concentration 0.1 mM and incubated for 4 hours. OD600 of the culture was measured and 1 OD was collected by centrifugation 5,000 rpm for 5 minutes. The cell pellet was re-suspended with 50 ml of distilled water and 20 ml of 4X sample buffer. The 0.1 OD of cell suspension was loaded in 10% SDS-PAGE.

#### 2.2 Protein Electrophoresis

Sample Preparation: Protein sample was prepared by mixing 4X sample buffer (4 mM EDTA, 200 mM Tris-HCl pH 7.5, 4% (w/v) SDS, 40% glycerol, 1.45 mM Bromophenol blue, 100 mM DTT) at the 1:3 ratio, vortexed and then boiled for 5 minutes. The sample mixture was centrifuged at 12,000 rpm for 5 minutes. The supernatant was loaded into wells of SDS-PAGE.

SDS-Polyacrylamide Gel Electrophoresis (SDS-PAGE): The mixture of saparating layer is 2.6% C, 10% or 15% T, 0.375 M Tris-HCl pH 8.8 and 0.1 % SDS. The stacking layer contained 2.6% C, 4% T, 0.125 M Tris-HCl pH 6.8 and 0.1 % SDS. The running buffer is Tris-glycine buffer (25 mM Tris, 192 mM glycine, 0.1% SDS). The electrophoresis was performed in constant voltage 100 Volts at room temperature until the dye reached the bottom of the gel. The protein bands were visualized by staining the gel in staining solution

(50% methanol, 10% glacial acetic acid, 0.1% Coomassie Brilliant Blue R-250 in water) for 1 hour on orbital shaker. The gel was then destained in 10% methanol, 10% glacial acetic acid overnight or until the background was clear.

#### 2.3 Partial Purification of Protein Inclusions

After toxin expression, The cell was collected by centrifugation 6,000 rpm for 10 minutes and re-suspended with distilled water. The cell suspension was lyzed by French Pressure Cell at 18,000 psi to obtain the proteins. The pellet contained inclusion proteins, insoluble materials from lysed cell was isolated by centrifugation at 10,000 rpm 4°C for 15 min, then re-suspended in 1 ml of distilled water and sonicated at 3 seconds intervals for 15 minutes. The suspension was centrifuged at 10,000 rpm 4°C for 10 minutes. The cell debris, which was on the upper part of the pellet, was removed by using micropipette. In washing step, the pellet was again re-suspended in ice-cold distilled water and then collected at the same condition of centrifugation. The pellet was washed for 3-4 times or until the pellet was clean. Both cell lysate and partial purified protein inclusions were examined on 10% SDS-PAGE.

#### 2.4 Protein Quantification

Protein concentration of partial-purified inclusion was determined by using Bio-Rad protein assay reagent based on method described by Bradford (85). The Bovine Serum Albumin (BSA) was used as protein standard for calibration curve. The concentrations of BSA were prepared with distilled water from 0.1, 0.2, 0.4, 0.6, and 0.8 mg/ml. A 10 ml of either standard BSA or partial-purified inclusion was mixed with 300 ml of Bradford dye reagent and the mixture was further incubated at room temperature for 10 minutes. The absorption at 595 nm was measured by using Hitachi U-2000 spectrophotometer. The protein concentration was calculated from standard curve.

#### 2.5 Solubilization of Toxins

Inclusion protein was dissolved in 50 mM of carbonate buffer pH 9.8 (NaHCO<sub>3</sub>/Na<sub>2</sub>CO<sub>3</sub>) to make a final concentration 1 mg/ml. The suspension was incubated at 37 °C for 1 hour and the supernatant was collected by centrifugation at 10,000 rpm for 10 minutes. For solubility test, the concentration of pre- and post-centrifugation of protoxin were determined before loaded on 10% SDS-PAGE.

## 2.6 Proteolytic Processing of Protoxins

Soluble protoxin was treated with TPCK treated trypsin (N-Tosyl-L-phynylalanine Chloromethyl Ketone treated, Sigma) at the ratio protein:trypsin 20:1 w/w. The mixture was incubated at 37°C for 14-16 hours and then the trypsin digestion pattern was analyzed on 13% SDS-PAGE.

### 2.7 Protein Purification by Gel Filtration Chromatography

The activated toxin was purified by FPLC system (Amersham Pharmacia Biotech, USA) using Superdex 200 HR 10/30 column to separate the proteins by their sizes. The column was equilibrated with 50 mM NaHCO<sub>3</sub>/Na<sub>2</sub>CO<sub>3</sub>, pH 9.8 at the flow rate 0.4 ml/minute. The purification profile was observed under the UV absorbance of 280 nm. Both buffer and protein sample were filtered through 0.2 mm membrane before applied to the column. The corresponded peaks were collected and then analyzed on 13% SDS-PAGE.

## 2.8 Protein Concentration Assay

For spectroscopic analysis, the protein concentration was determined based on the absorbance at 215 and 225 nm (86). The protein spectrum was measured from 190 to 350 nm and subtracted with baseline spectrum. Protein concentration was calculated by the formula: Protein concentration (mg/ml) =  $0.144 \times (OD_{215} - OD_{225})$ , when pathlength of cuvette = 1 cm.

#### 3. Structural Characterization

## 3.1 Intrinsic Fluorescence Spectroscopy

Fluorescence spectra were obtained by emission scanning of protein solution (20 mg/ml in 50 mM NaHCO<sub>3</sub>/Na<sub>2</sub>CO<sub>3</sub>, pH 9.8) using RF-5301PC spectrofluorometer at the excitation wavelength 280 nm. The emission wavelengths were observed from 300 to 520 nm. The scanning rate was 50 nm/min, excitation and emission slit 5.0 nm. One spectrum was averaged from 3-4 scans. All spectrum were subtracted with baseline.

#### 3.2 Protein Unfolding by Guanidine Hydrochloride

Guanidine Hydrochloride (GuHCl, MW 95.5) is a hygroscopic compound, its molarity was determined by refractive index measurements. To prepare 100 ml of 8 M GuHCl in 50 mM NaHCO<sub>3</sub>/Na<sub>2</sub>CO<sub>3</sub> pH 9.8, the amount of GuHCl was calculated by using its MW and

solubilized in 40 ml of 50 mM NaHCO $_3$ /Na $_2$ CO $_3$ , pH 9.8. The molarity of GuHCl can be calculated from the equation (87, 88):

Molarity = 
$$57.147(\Delta N) + 38.68(\Delta N)^2 - 91.60(\Delta N)^3$$

Where  $\Delta N$  is the difference value of refractive index between the denaturant solution and buffer.

For unfolding experiment, 8 M GuHCl was diluted to the final concentrations from 0-5.29 M. Purified active toxin was mixed with the various concentrations of GuHCl and further monitored by using intrinsic fluorescence spectroscopy. The unfolding curves were constructed by using intensity ratio 340/350 nm for each samples. These curves were fit with the unfolding equation to obtain mid point value, which is the molarity of GuHCl that can unfold half part of protein (89-91).

$$f_{\text{app}} = (\alpha_{\text{N}} + \beta_{\text{N}} [\text{GuHCI}]) + (\alpha_{\text{U}} + \beta_{\text{U}} [\text{GuHCI}]) \exp^{[m([\text{GuHCI}] - [\text{GuHCI}]^{50\%})]/\text{RT}}$$

$$1 + \exp^{[m([\text{GuHCI}] - [\text{GuHCI}]^{50\%})]/\text{RT}}$$

 ${\it f}_{\rm app}$  is apparent fraction unfolded (F340/F350),  $\alpha_{\rm N}$  and ( $\alpha_{\rm U}$  are the Y-intercept of native and unfolded state,  $\beta_{\rm N}$  and  $\beta_{\rm U}$  are the slope of native and unfolded state, respectively. m is the GuHCl index, [GuHCl] is the mid point value. The different of free energy value ( $\Delta {\it G}^{\circ}_{\it W}$ ) between native and unfolded state is calculated by the equation:

$$\Delta G^{\circ}_{W} = m \times [GuHCI]^{50\%}$$

## 4. Mosquito Larvicidal Assay

The 2 day-old *Aedes aegypti* mosquito larvae were obtained from the mosquito-rearing facility of the Institute of Molecular Biology and Genetics, Mahidol University. The cell culture of 10 OD was collected by centrifugation 5,000 rpm for 10 minutes. The cell pellet was re-suspended with 2 ml of distilled water. The larvae were counted on 48-well titration plate (11.3 mm well diameter, Costar, MA, USA). 10 wells were performed for either wild type or mutant. Each well contained 10 larvae and was added with 200 ul (1 OD) of cell suspension. The larvae were counted after 24 hours incubation at room temperature.

#### **RESULTS AND DISCUSSIONS**

## 1. Expression and Purification of Toxins

The *Bacillus thuringiensis spp. Israelensis (Bti)* wild type Cry4B protein and its mutant were produced by expressing the pMU388 DNA plasmid in *E. coli* JM109 under an induction of 0.1 mM IPTG at 37°C. The protein product was produced as an inclusion body. The preliminary characterization of the crude protein showed that the toxin is insoluble in distilled water but well soluble in 50 mM NaHCO<sub>3</sub>/Na<sub>2</sub>CO<sub>3</sub>, pH 9-10. SDS-PAGE analysis gave an intense band of protoxin around 130 kDa (Figure 3). Further processing of protoxin by trypsin yielded an active form of toxin containing 47- and 18-kDa fragment on SDS-PAGE. These two fragments were previously found to be tightly associated as a 65-kDa molecule in the native buffer condition. In this work we avoid a complication of data interpretation resulting from association and dissociation of the two fragments by creating a R203Q mutant. This mutant toxin has no tryptic site at the R203 position giving a single fragment of active toxin of 65 kDa (Figure 4). This mutant was then used as a reference or template for all other mutants.

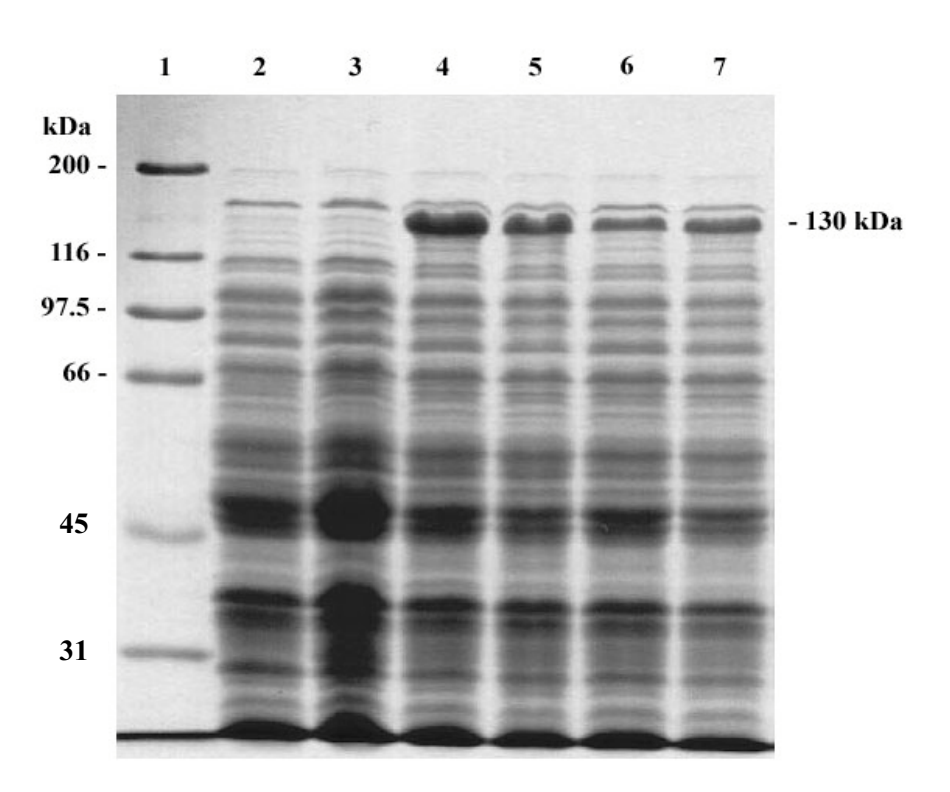


**Figure 3:** SDS-PAGE Analysis of the 130-kDa protoxin products (1) standard protein marker (2) JM109 cell with pUC12 (4-5) JM109 expressing Cry4B and (6-7) JM109 expressing R203Q

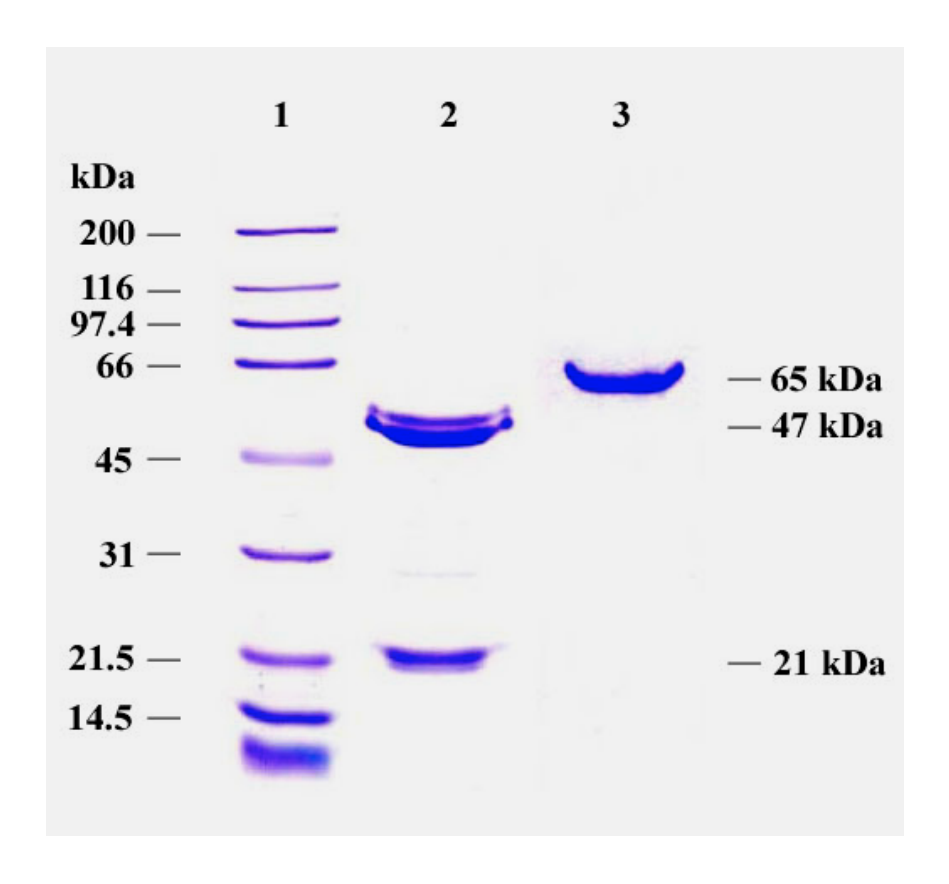
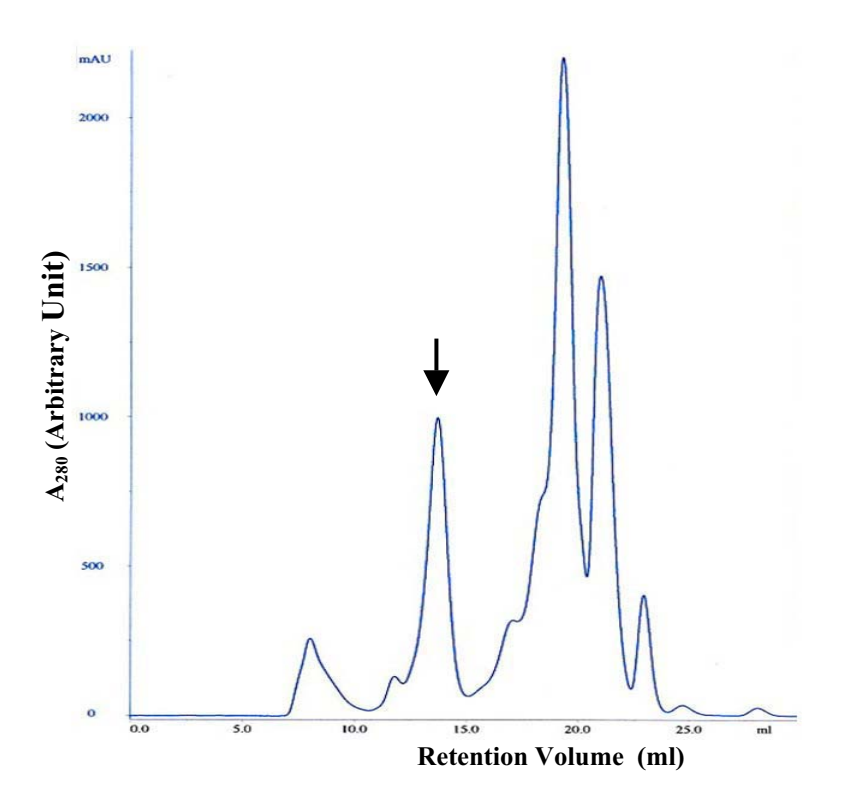
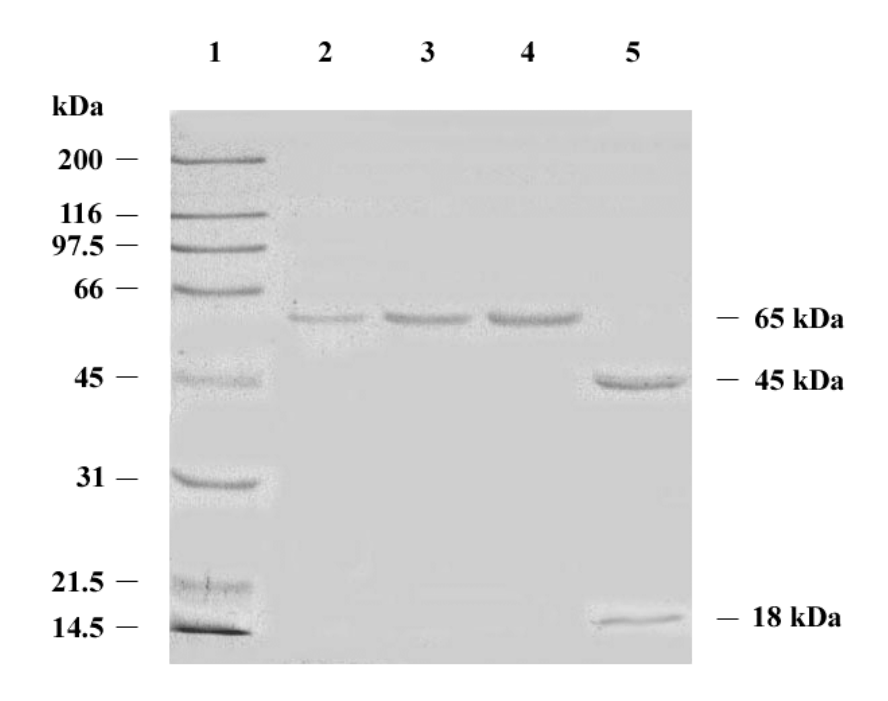


Figure 4: SDS-PAGE analysis of the proteolytic processed products
(1) standard protein marker (2) wild type Cry4B and (3) R203Q mutant

After proteolytic processing of protoxins, the 65-kDa active toxins were obtained by size- exclusion chromatography. Superdex-200 HR 10/30 semi-preparative column (Amersham) was employed with flow rate around 0.4-0.5 ml/min in carbonate buffer pH 10. The purified protein fraction was obtained from chromatographic peak around 14 ml (Figure 5). The chromatographic purified fraction gave a single band of protein of 65 kDa for R203Q and two protein bands around 18 and 45 kDa for wild type on SDS-PAGE analysis(Figure 6). Molar concentration of the stock protein was determined based on Bradford and UV absorption.



**Figure 5**: Typical chromatographic profile of the proteolytic processed toxin. The 65 kDa active molecule is eluted out at elution volume around 14 ml (noted with arrow)



**Figure 6:** SDS-PAGE analysis of the purified toxin (1) standard protein marker (2-4) R203Q and (5) Wild type Cry4B

## 2. Characterization of Wild Type Cry4B and R203Q Template

The purified Cry4B toxin and the tryptic site removed mutant, R203Q were characterized by an unfolding experiment. The 65-kDa active toxins in alkali carbonate buffer were gradually induced from the native state to the unfolded state by a series of guanidine hydrochloride (GuHCI) concentrations.

# 2.1 Steady-State Unfolding:

After an incubation of the native toxin in a series of GuHCI, a conformational change was clearly detected by circular dichroism and fluorescence spectroscopy. According to the CD spectra, toxin in the native state showed a well-defined CD spectrum containing an intense positive band around 193 nm and a broad negative band around 210-220 nm. These characteristics suggest a mixed portion of alpha helix and beta strand conformations (Figure 7). Based on an estimation of secondary structure of this active toxin from x-ray structure, the content of alpha and beta are somewhat similar at around 30-40% for each conformation. In the presence of GuHCI which is highly absorpt the UV-light, a reliable measurement was allowed to go down to only 210-215 nm. However a conformational change was found as the CD spectra showed a decreasing of the negative band intensity upon an increasing of GuHCI concentration. This feature indicates a loss of protein secondary structure. These spectral changes are found typical for both wild type Cry4B and R203Q mutant.

The intrinsic fluorescence spectra of toxins also revealed a conformational change of protein from native to unfolded state. These spectra showed a red shift of  $\lambda$ max from 340 to 350 nm and reduced intensity when the denaturant concentration is raised (Figure 8). The feature reflects the loose packing of protein tertiary structure towards an unfolded state. These spectral changes were also found typical for wild type and mutants.

## 2.2 Determination of Unfolding Free Energy

Changes of spectral intensity in CD measurement and shifting of the fluorescence spectra ( $\lambda$ max) were employed for a construction of an unfolding curve for each toxin. Based on CD spectra we have established the maximum and minimum intensity around the band at 222 nm for the fully folded (native) and the fully unfolded conformation. The plot was depicted in terms of fraction unfolded of protein for various concentrations of denaturant..

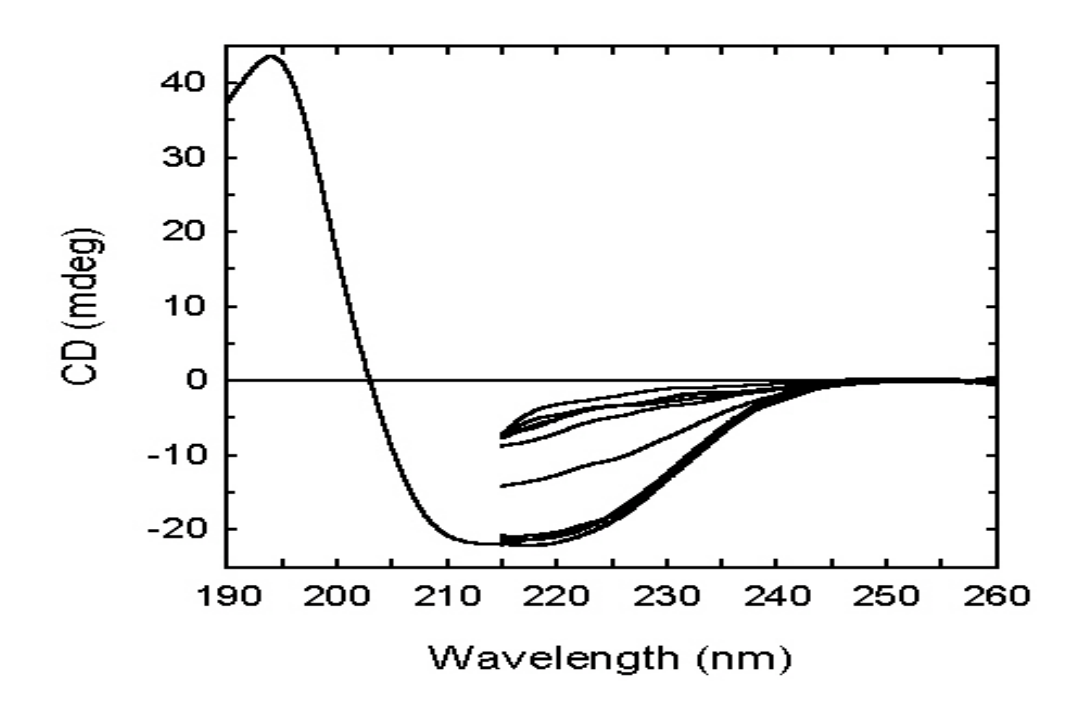


**Figure 7:** A typical changes of circular dichroism spectra of toxin in various concentrations of GuHCl

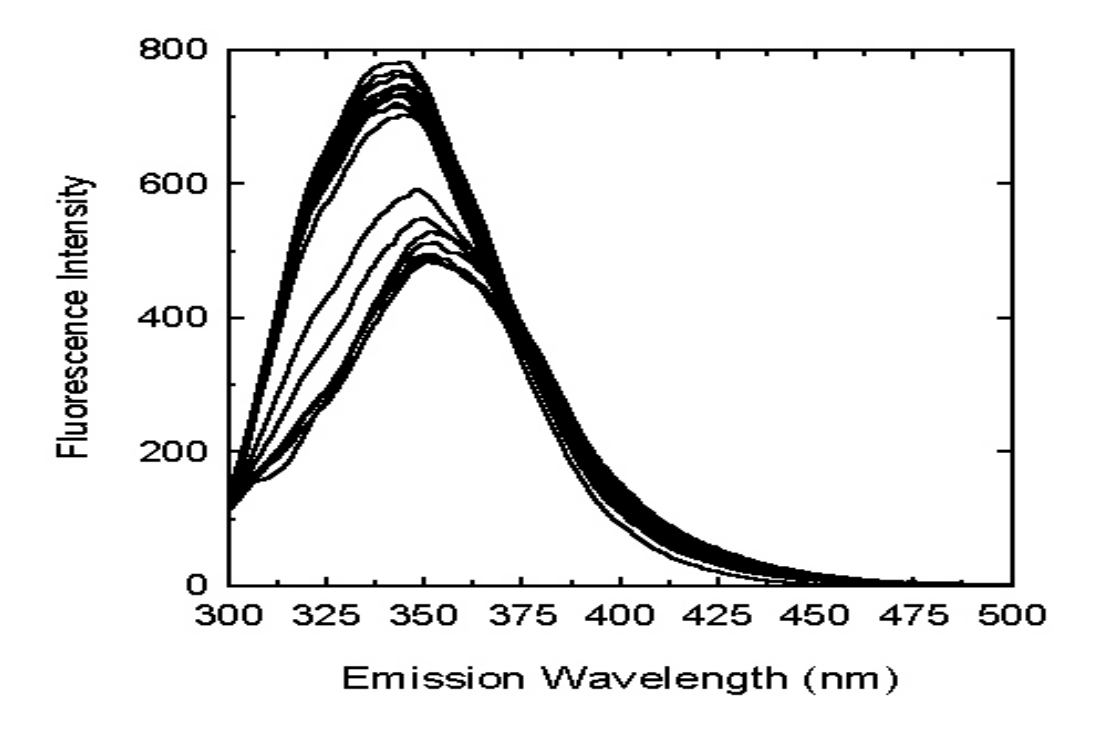
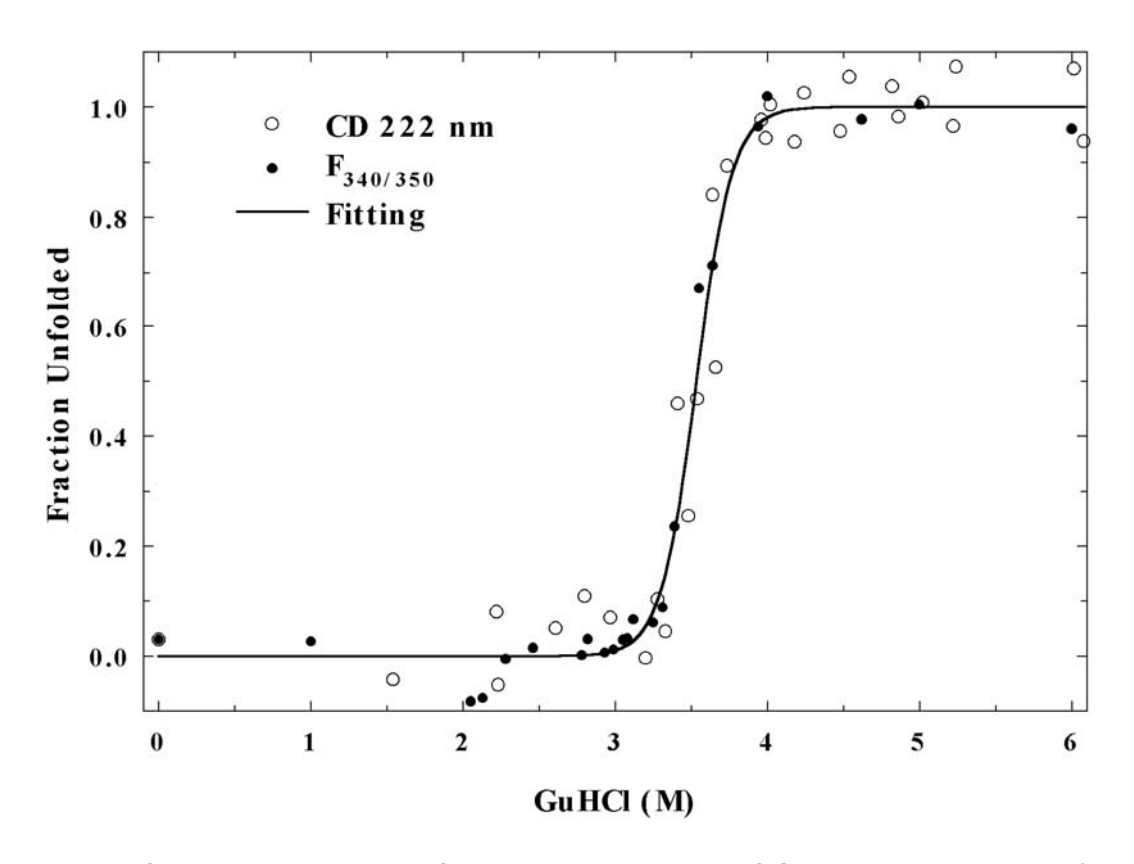


Figure 8: A typical changes of intrinsic fluorescence spectra of toxin in various concentrations of GuHCI

An unfolding curve was also construct from the fluorescence data. Based on the changing feature of the fluorescence spectra, we plot the fraction unfolded by using an intensity ratio between two wavelengths, 340 and 350 nm.

Unfolding curves for both wild type and the mutants reveal a two-state transition from native to unfolding states. The plots demonstrate the transition with a sigmoidal characteristic with conformational transition located in a narrow range (around 0.5-1.0 M) of GuHCl concentration. The transition is rapid and there was apparently no sign of stable intermediate. Interestingly, the curves derived from both CD and fluorescence spectra were found identical (Figure 9). Our method independent result can be used as a strong confirmation for the two-state model.



**Figure 9:** Unfolding curves derived from intensity changes of CD spectra at 222 nm (open circle) and fluorescence intensity ratio between 340/350 nm (close circle)

According to the unfolding curve of wild type Cry4B, curve-fitting analysis by a two-state model equation was performed. An analysis yielded a transitional midpoint ([GuHCl]<sup>50%</sup>) at 3.53 M and the transitional slope (m) of 5059 cal/mol M. The unfolding free energ ( $\Delta$ G) obtained from a multiplication of these two parameters can be reported at 17.86 kcal/mol.

This free energy value represents the amount of energy required for a transition from native or folded state to the unfolded state. In general this reported energy can also be used to indicate a structural stability of the native protein. Based on a current database for conformational free energy of proteins, the values are found in a wide range. However most of the characterized proteins are reported with the values around 5-20 kcal/mol.

The R203Q mutant was also characterized in paralleled with our wild type toxin. We found a similar sigmoidal unfolding curves. However a comparison with wild type toxin revealed a conformational transition shifted to a higher concentration of denaturant. This feature obviously suggests a higher stability of the native state of mutant (Figure 10).

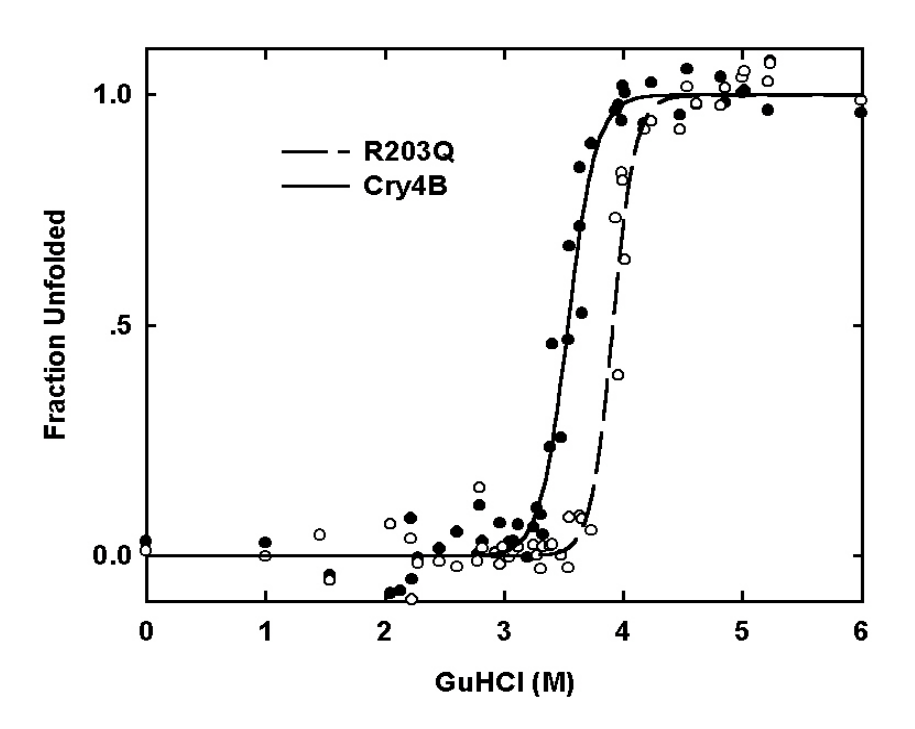


**Figure 10**: A comparison of unfolding curves obtained from wild type (close circle) and R203Q mutant (open circle)

Our model fitting analysis of R203Q yielded a transitional midpoint ([GuHCl]<sup>50%</sup>) at 3.92 M and the transitional slope *(m)* of 5890 cal/mol M. Therefore, the unfolding free energy ( $\Delta$ G) obtained from a multiplication between these two parameters can be reported at 23.09 kcal/mol. The difference in unfolding free energy between R203Q and wild type Cry4B is defined as  $\Delta\Delta$ G = 5.23 kcal/mol. The enhanced stability of R203Q is suggested to be due to

a removal of the tryptic site at the position 203, resulting in a single chain molecule of 65-kDa relative to the associated fragment of 18 and 47-kDa in wild type toxin. The similar effect has been found in several proteins and dimers introduced with additional covalent bond.

Since our research here will continue with an analysis for the effect of mutation of stabilizing residues and bonding, we will employ the single chain R203Q as a template for further mutagenesis study. Our selection of R203Q would avoid a complication of data analysis contributed from a dissociation/association between the two fragments of the original wild type. Moreover, those mutational effects would be determined relative to the template molecule and still reliable.

In summary we have determined unfolding free energy of wild type and R203Q mutant in a steady state (equilibrium) unfolding experiment. These unfolding free energy are 17.86 and 23.09 respectively.

# 2.3 Analysis of Unfolding Kinetics

Our kinetics study is involved with the real time monitoring of the conformational changes from native to unfolded state. According to the fluorescence intensity at 340 nm, which is the  $\lambda$ max for the native state, we observed a rapid exponential decay of spectral intensity when the toxin as mixed with denaturant. The decay rate of intensity was found to be dependent to the final concentration of the mixed denaturant (Figure 11). Assuming that the conformational change is dealing with an intra-molecular interaction, we have analyzed the data by using the first-order kinetic model. The analysis has revealed an unfolding rate  $(k_{\text{obs}})$  of protein from native to unfolded state at each denaturant concentration.

Since our final aim of kinetics study is to obtain the unfolding rate constant ( $k_{\rm obs}$ ) of the toxin in the native condition without denaturant, a plot between a logarithm of  $k_{\rm obs}$  ( $\ln k_{\rm obs}$ ) versus denaturant concentrations was performed and extrapolated to the condition of 0 M GuHCl (Figure 12).

An unfolding rate constant in an absence of denaturant ( $k^{0}_{U,W}$ ) for wild type Cry4B and R203Q was calculated and reported. We found that the calculated unfolding rate constant of wild type and R203Q are almost identical (8.82 x  $10^{-7}$  and 8.90 x  $10^{-7}$  sec<sup>-1</sup> respectively) These rate constant are rather slow as we can see the completion of the conformational changes ranging from 100 - 500 seconds (Figure 11).

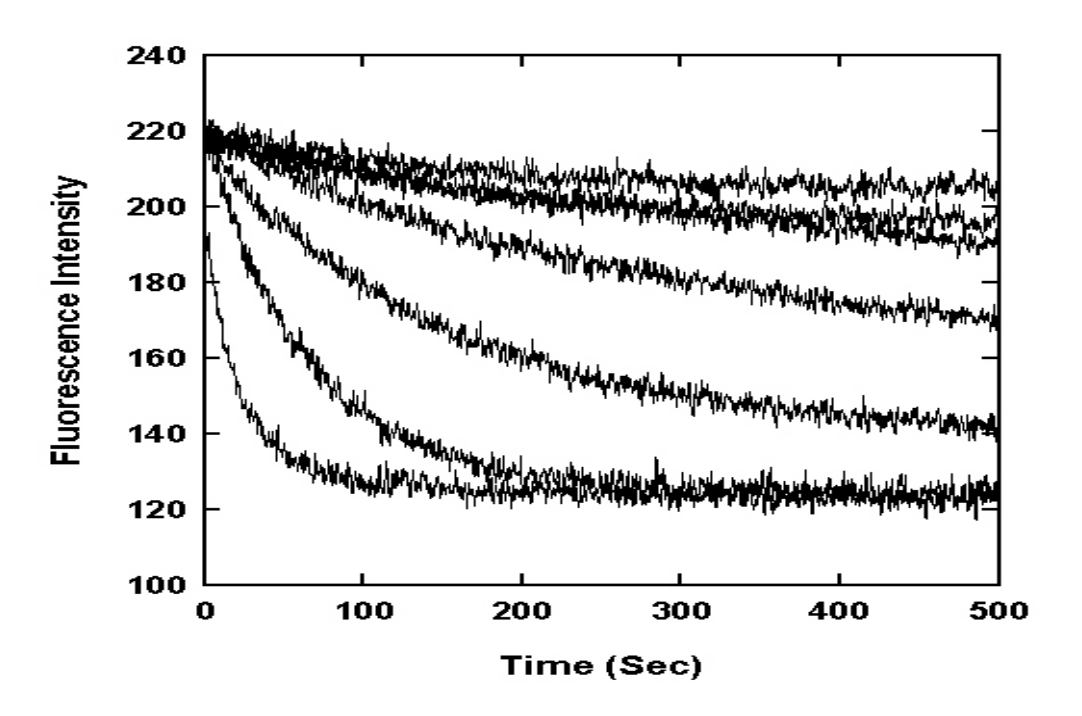


**Figure 11**: A trypical exponential decay of the fluorescence intensity at 340 nm during the unfolding kinetics study under various concentrations of denaturant

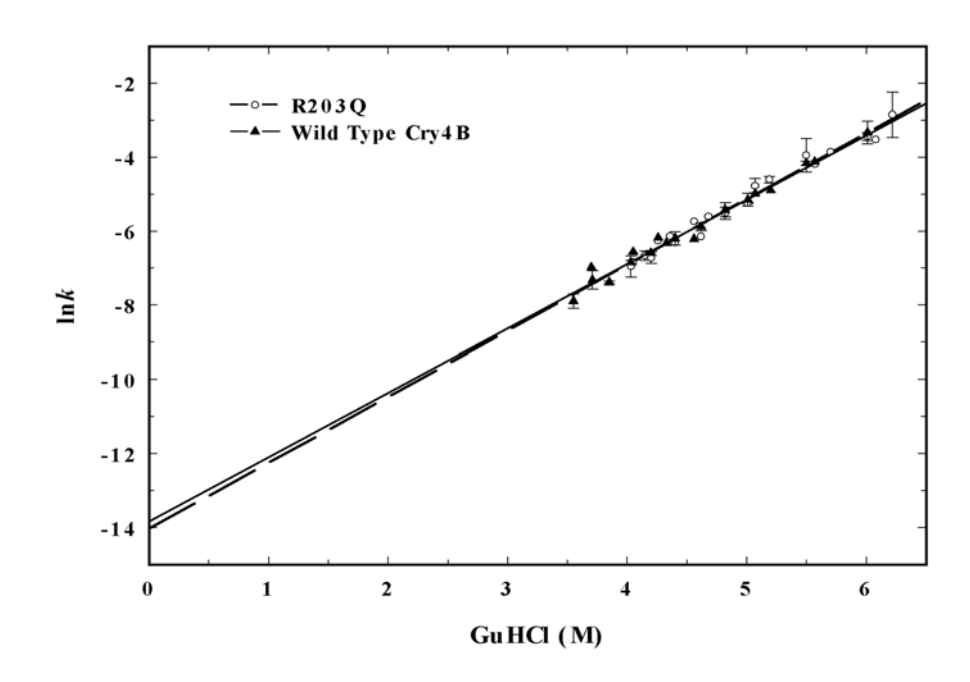


**Figure 12:** Plots of  $\ln k_U^{\circ}$  and denaturant concentrations reveal a linear relationship. Error bars indicate standard error from 3 independent experiments. Y-intercept  $(\ln k_{U,W}^{\circ})$  from linear extrapolation is -14.04± 0.34 for wild type and -13.94 ± 0.09 for R203Q, respectively.

## 2.4 Determination of Transitional Activation Energy

Based on the unfolding rate constant  $(k^{\circ}_{U,W})$  obtained from our kinetics study, an activation energy of unfolding in the absent of denaturant  $(Ea^{\circ}_{U,W})$  can be calculated using an equation:

$$k_{U,W}^{0} = (k_{B}T/h)exp^{(-Ea_{U,W}^{0})/RT}$$

We found that the activation energies of unfolding are nearly the same for both wild type and R203Q (25.77 and 25.71 kcal/mol, respectively). These energies are list in Table 1.

Toxins	$\ln k^{\circ}_{\mathrm{U,W}} \pm \mathrm{SEM}^{/1}$	$k^{o}_{U,W} \pm SEM$ (×10 <sup>-7</sup> s <sup>-1</sup> )/2	Ea° <sub>U,W</sub> ± SEM (kcal/mol) /3
Cry4B	-14.04 ± 0.34	8.82 ± 2.61	25.77 ± 0.20
R203Q	-13.94 ± 0.09	8.90 ± 0.85	25.71 ± 0.06

Table 1: Kinetics parameters from unfolding kinetics of Cry4B and R203Q

## 2.5 Construction of Energy Map

A construction of an energy profile of protein unfolding requires a combined data from steady state and kinetics experiments. In steady state experiment, we have calculated protein unfolding free energy ( $\Delta G$ ) which reflects an energy gap between the native and unfolded state. While the kinetic experiment yielded an activation energy (Ea) that represents an energy barrier of the transition state. These two parameters were then plot against reaction coordinates from native (N), transition state (TS) and the unfolded state (U). The energy map for Cry4B and R203Q are depicted in Figure 13.

From the energy map, one can see that the energy gaps between native and unfolded state are 17.86 and 23.09 kcal/mol for wild type and R293Q respectively. These free energy gaps are thermodynamically controlled or process independent. The energy level

for the native state of R203Q is located at 5.23 kcal/mol lower than that of the wild type while the energy for their unfolded state are the same. However an activation energy of both wild type and R203Q is identical. This energy map, especially for R203Q is used as a template for further characterization of other mutants.

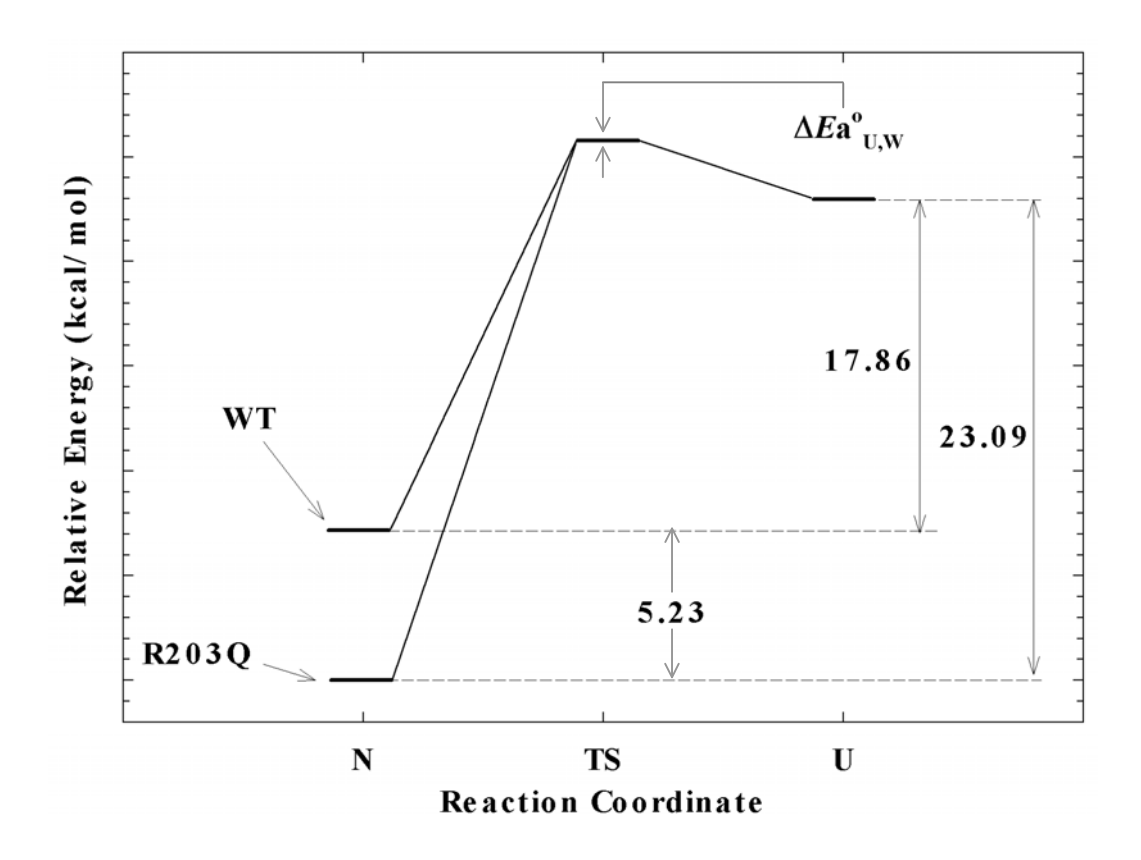


Figure 13: Energy map showing reaction coordinates and their energy levels.

# 3. Site-Directed Mutagenesis

## 3.1. Construction of Mutant Plasmids

The selected conserved amino acid residues located in the conserved blocks were subjected to be investigated by changing to other amino acids. The resulting mutant plasmids are:

Group I : pL175V, pl189L

Group II : pR251A, pD259N, pY267F, pT285V, pH466Y, pD470N, pK487A,

pR627A and pE629Q,

These mutants were obtained by site-directed mutagenesis using pR203Q as a template. The synthetic oligonucleotide primers were designed to direct for those mutations. The 6.3-kb PCR products were successfully obtained and digested with *DpnI* to remove the parental DNA template. The amplification bands of 6.3-kb DNA from PCR were illustrated on a single band on agarose gel electrophoresis as shown in Figure 14 to 15.

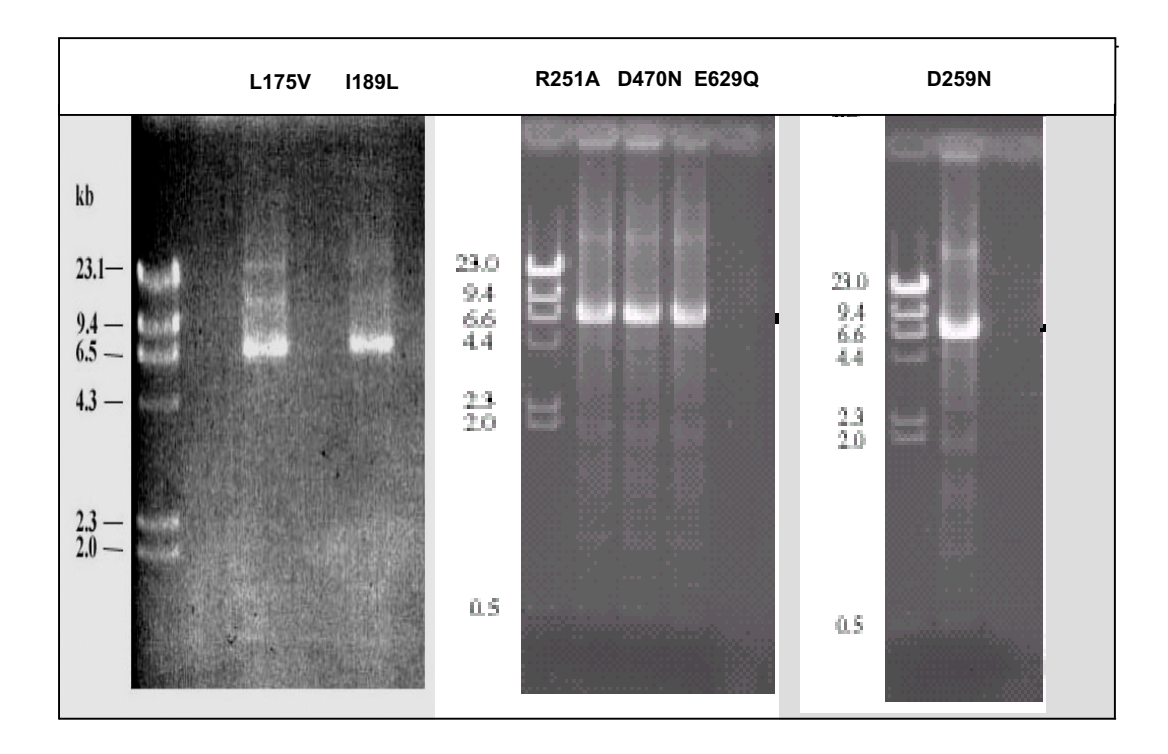


**Figure 14:** Agarose gel electrophoresis analysis of L75V, I189L, R251A, D470N, E629Q and D259N mutant plasmids from PCR

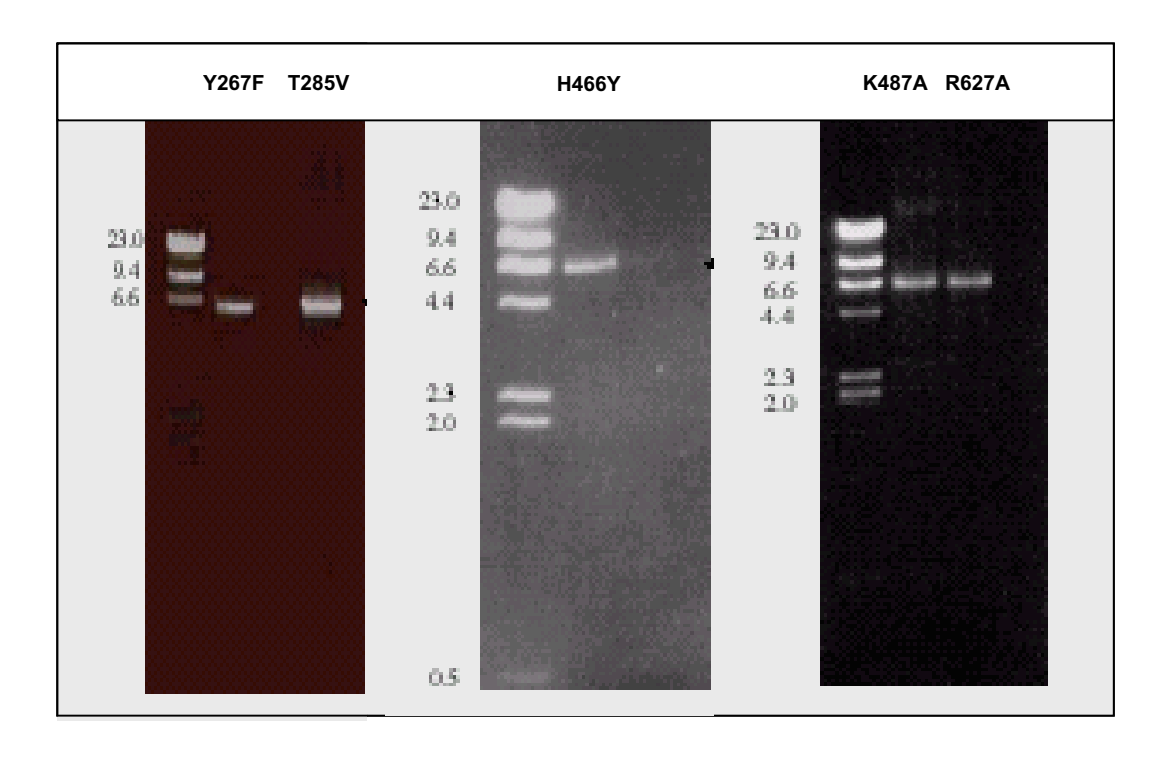


**Figure 15:** Agarose gel electrophoresis analysis of Y267F, T285V, H466Y, K487A and R627A mutant plasmids from PCR

## 3.2. Restriction Endonuclease Analysis of Plasmids

The *DpnI*-treated PCR products were transformed into competent *E. coli* JM109 by heat shock method as previously described. The transformants were screened to distinguish between template and mutants using restriction endonuclease analysis. The restriction endonucleases were selected following the recognition site in synthetic oligonucleotide primers.

The different DNA digestion patterns of pR203Q template and its mutants, pL175V, pl189L, pR251A, pD259N, pY267F, pT285V, pH466Y, pD470N, pK487A, pR627A and pE629Q, are shown in Figure 16 to 26, respectively. The automated DNA sequencing chromatograms of the selected mutant clone are also confirmed the correct sequence and shown in the figures.

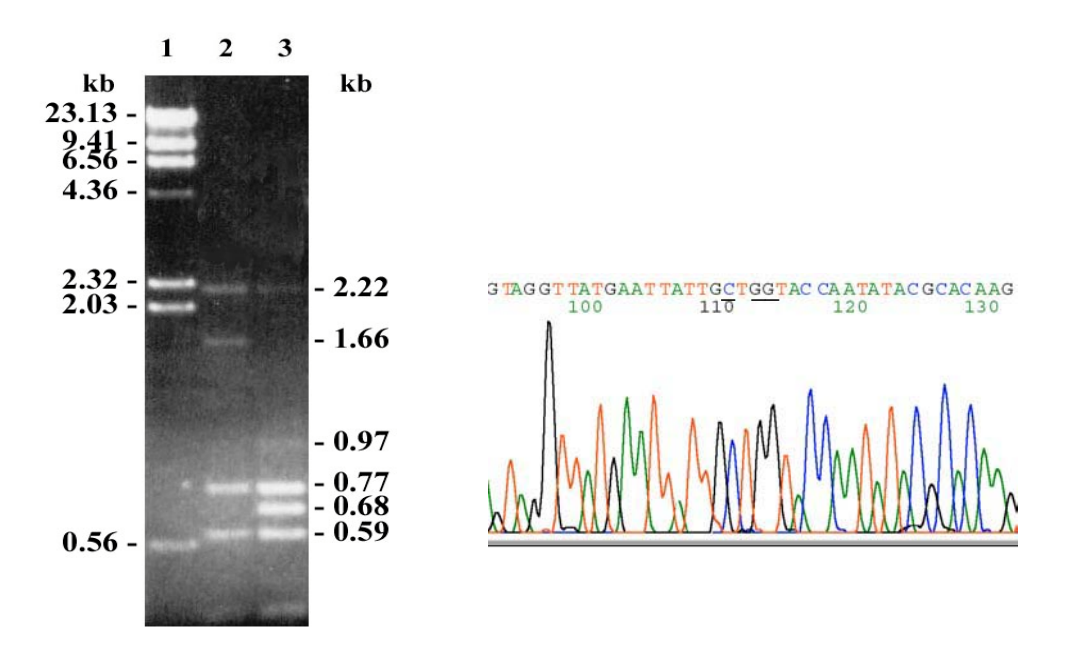


Figure 16: Restriction analysis and sequence confirmation of pL175V

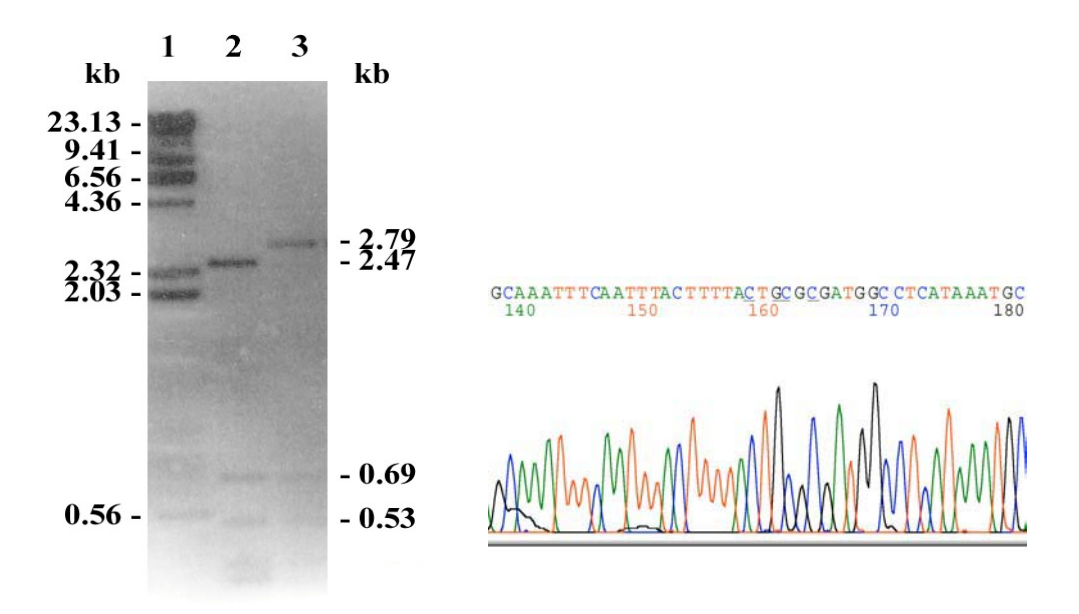


Figure 17: Restriction analysis and sequence confirmation of pl189L

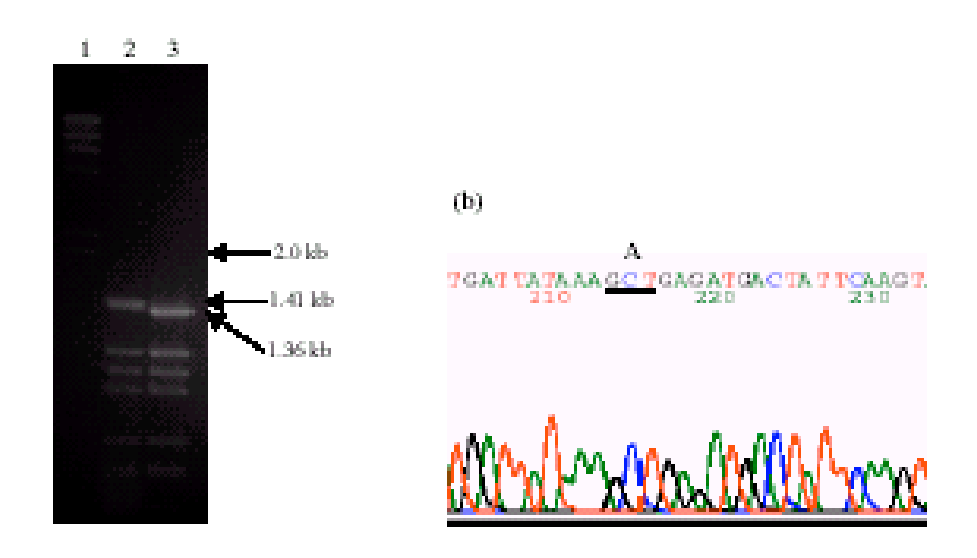


Figure 18: Restriction analysis and sequence confirmation of pR251A

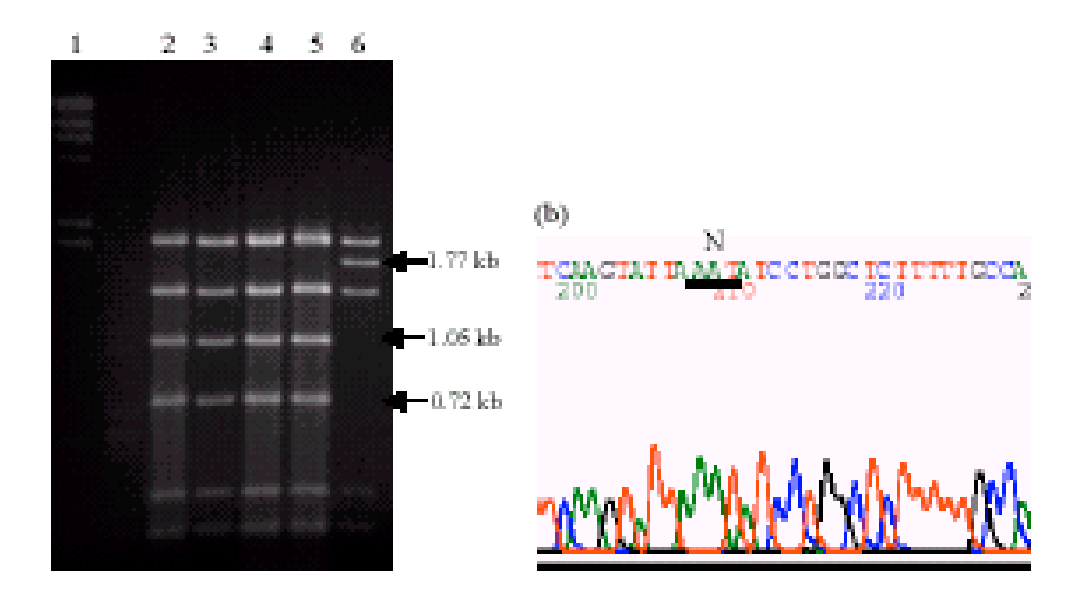


Figure 19: Restriction analysis and sequence confirmation of pD259N

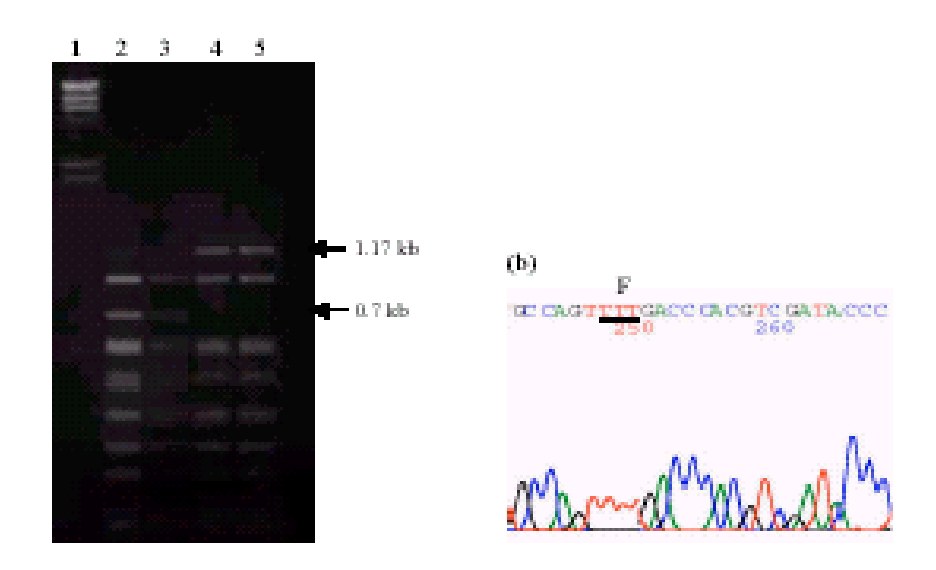


Figure 20: Restriction analysis and sequence confirmation of pY267F

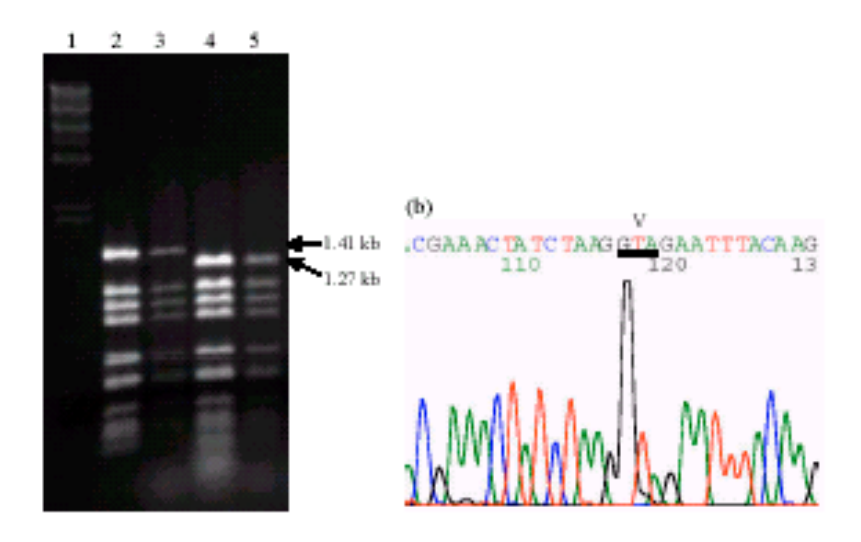


Figure 21: Restriction analysis and sequence confirmation of pT285V

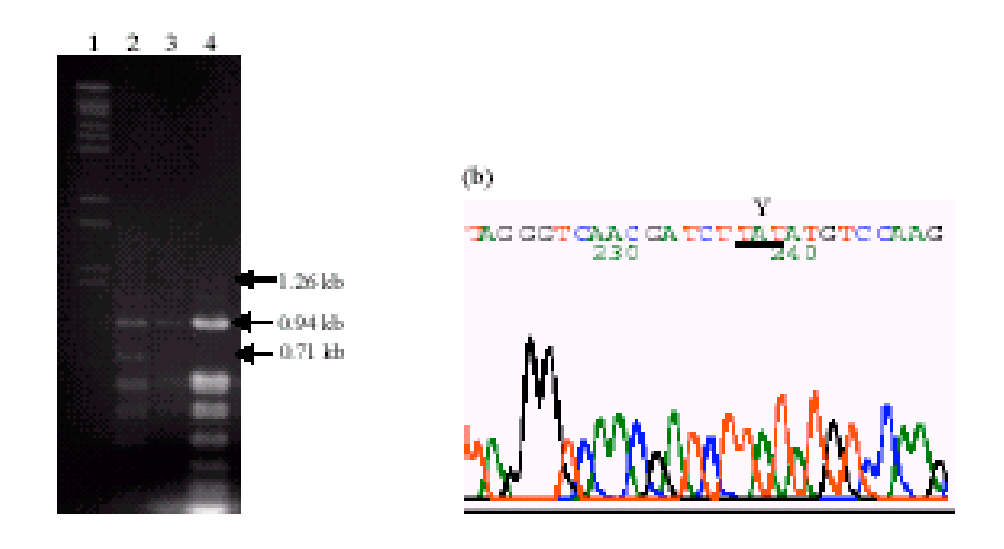


Figure 22: Restriction analysis and sequence confirmation of pH466Y

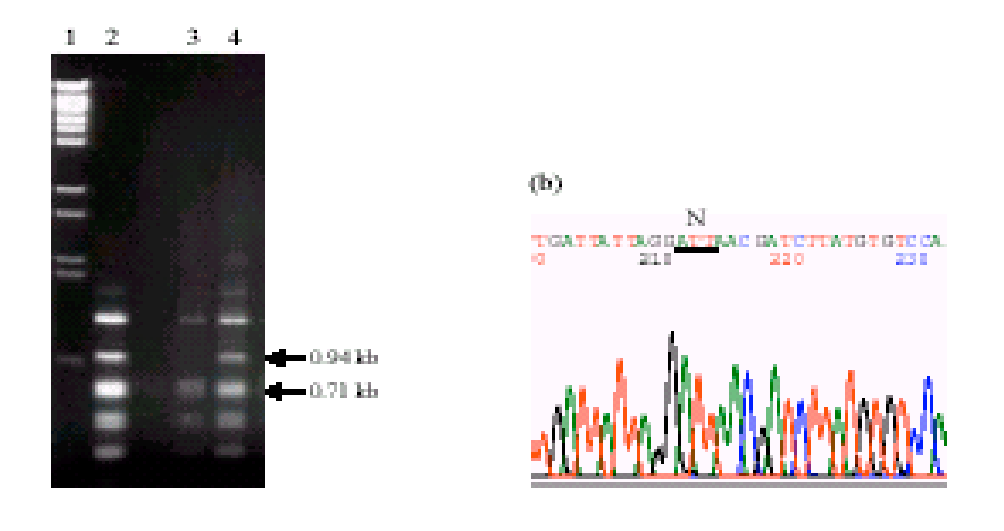


Figure 23: Restriction analysis and sequence confirmation of pD470N

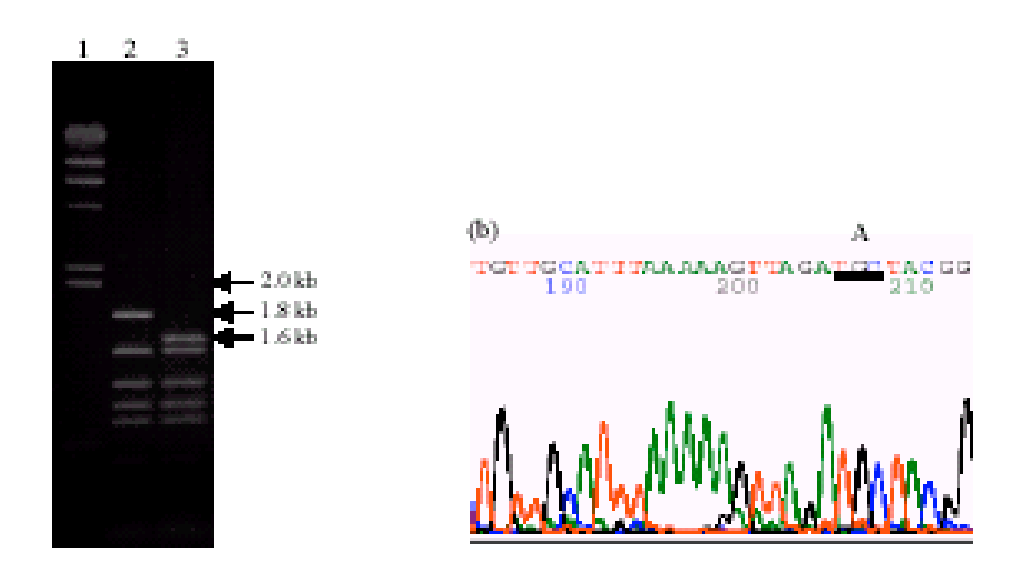


Figure 24: Restriction analysis and sequence confirmation of pK487A

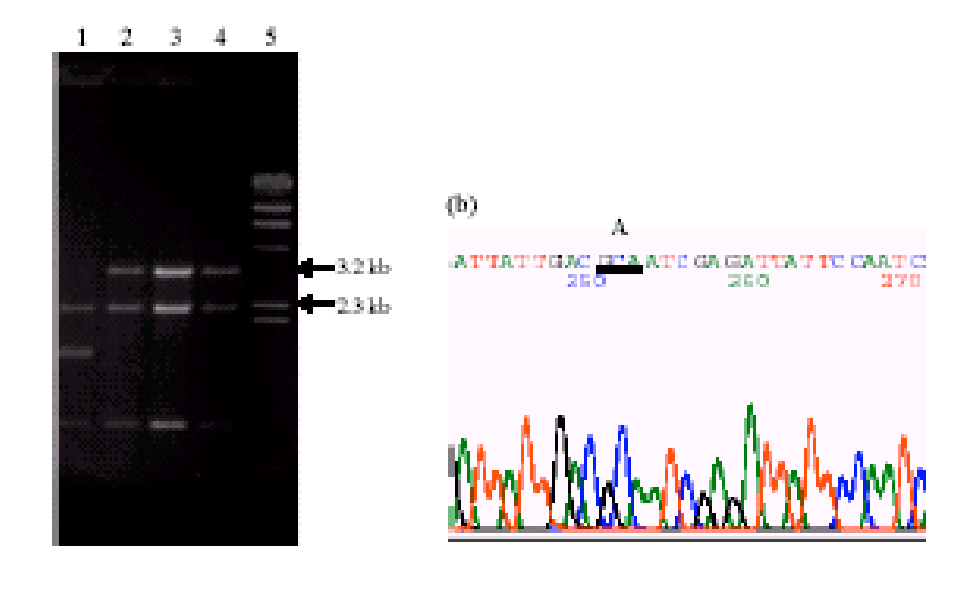


Figure 25: Restriction analysis and sequence confirmation of pR627A

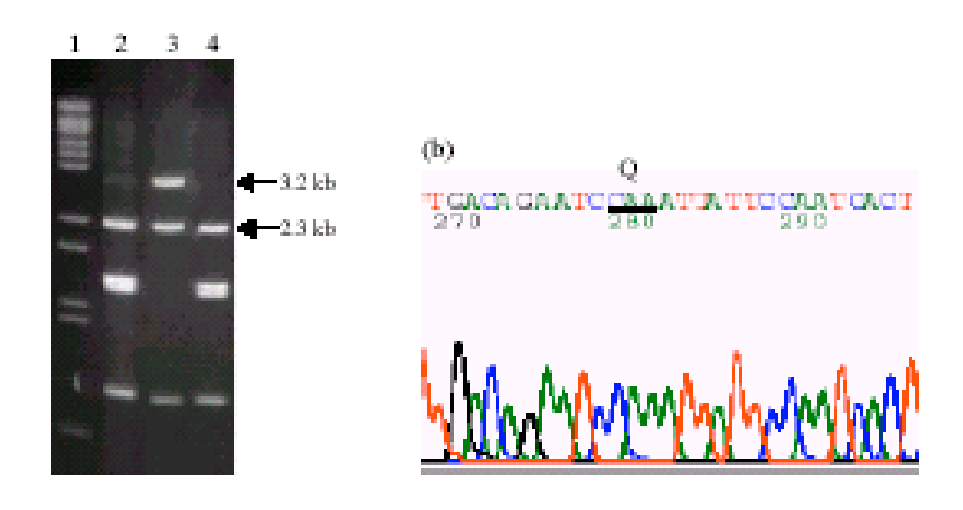
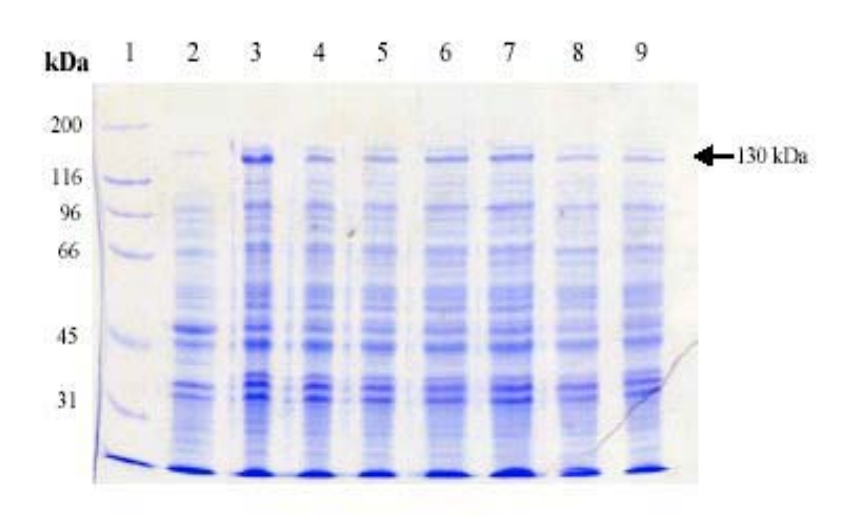


Figure 26: Restriction analysis and sequence confirmation of pE629Q

# 3.3. Expression and solubilization of Mutant toxins

All mutants were found to express for the 130-kDa protoxin under IPTG induction. Their expression levels were mostly the same as the R203Q template (Figure 27).



**Figure 27**: A typical expression profile of mutant toxin on SDS-PAGE showing the protoxin product at 130 kDa.

Our preliminary characterization was performed by measuring protein solubility in 50 mM NaHCO<sub>3</sub>/Na<sub>2</sub>CO<sub>3</sub>, pH 9.8. Interestingly, a numbers of mutant toxins were found to be insoluble in the native buffer condition. These mutants include D259N, Y267F, T285V, K487A and R627A. Since the R203Q template protein and original wild type are well soluble in the alkali carbonate buffer, a drastic change of solubility in these mutant toxins can be used as a strong indication for an incorrect folding of the native toxin structure. An explanation based on the selection of these mutated residues should be addressed in terms of loss in specific stabilizing forces or bonding. According to a x-ray structure of the active Cry4B, the residues D259, Y267, T285, K487 and R627 are the conserved residue lie within the five conserved blocks of toxin molecule, providing either hydrogen bond or salt bridge for structural stabilization. An important observation is that these stabilizing bonds and interaction were found between these mutated residues and residues located closely in space but far away in the linear sequence. Mutations that eliminate these stabilizing forces have a significant effect to the ability of protein to adopt the correct native conformation.

## 3.4 Proteolytic Processing of Soluble Toxins

The 130-kDa soluble template protein (R203Q) and L175V, I189L, R251A, H466Y, D470N, E629Q mutant toxins, were then subjected to proteolytic processing by trypsin to produce the 65-kDa active toxins. Upon an analysis by SDS-PAGE, it was found that the L175V, I189L, R251A, H466Y, and D470N mutants yielded the 65-kDa products similar to their R203Q template. While the E629Q mutant toxin gave no detectable product of a 65-kDa protein. Even though the E627Q mutant was found to be soluble in an alkali carbonate buffer like other, a complete digestion by trypsin has suggested that the soluble conformation of this mutant is somehow different from the native toxin. Therefore, the stabilizing interaction provided by this E627 residue is critical for the folding of native structure.

## 3.5. Chromatographic Purification of Mutants

The 65-kDa soluble R203Q template protein and its mutants, L175V, I189LR251A H466Y, D470N, were purified using size-exclusion column. All samples showed chromatographic profiles containing the 65-kDa product peak at retention volume approximately 13-14 ml. These purified fractions were confirmed in SDS-PAGE as a single band.

# 4. Characterization of Protein Unfolding for Mutants

Our basis for site-directed mutagenesis study is focused on a removal of hypothesized stabilizing forces provided by a numbers of residues within the conserved sequence blocks. These selected residues were chosen based on the examination on the three dimensional structure of Cry4B. We have started by an investigation of the hydrophobic interaction located on the conserved block I of domain I.

# 4.1. Roles of the Hydrophobic Interaction in conserved Block I

According to the structural feature of domain I which is a helical bundle among seven helices, we were interested in the highly conserved helix-5 located in the center of domain I. This central helix is surrounded by the other helices and it represents the conserved block I among the sequences of Cry toxins. The residues in this conserved block are mostly an amino acid with hydrophobic side chain. These hydrophobic residues should provide a suitable environment for structural packing in the core of domain interior. From other reports and our experiences in mutating a residue in this conserve block, these mutations usually lead to the expression of the insoluble protein product. These results has already confirmed the critical role of residues in this conserved block I on the formation of correct native folding. Here in this work we choose to make a rather conserved mutation from L175 to V and I189 to L. Our conservative changes among L, V and I has led to the expressed mutant proteins with comparable solubility to their template. The advantage of getting these mutant proteins in a soluble form is that they can be subjected to further analysis in protein unfolding experiment.

From basic characterization of the biochemical properties, the constructed L175V and I189L mutants were found to have a comparable expression level, solubility and proteolytic processing pattern to that of the R203Q template. This is a good indication that the mutants can fold into the native-like conformation. However, an unfolding experiment has revealed different unfolding curves between these two mutants (Figure 28). We found that the unfolding curve of L175V is shifted to the lower concentration of denaturant while I189L give an identical curve to the template protein. After model fitting analysis their transitional mid point and unfolding free energy were list in Table 2.

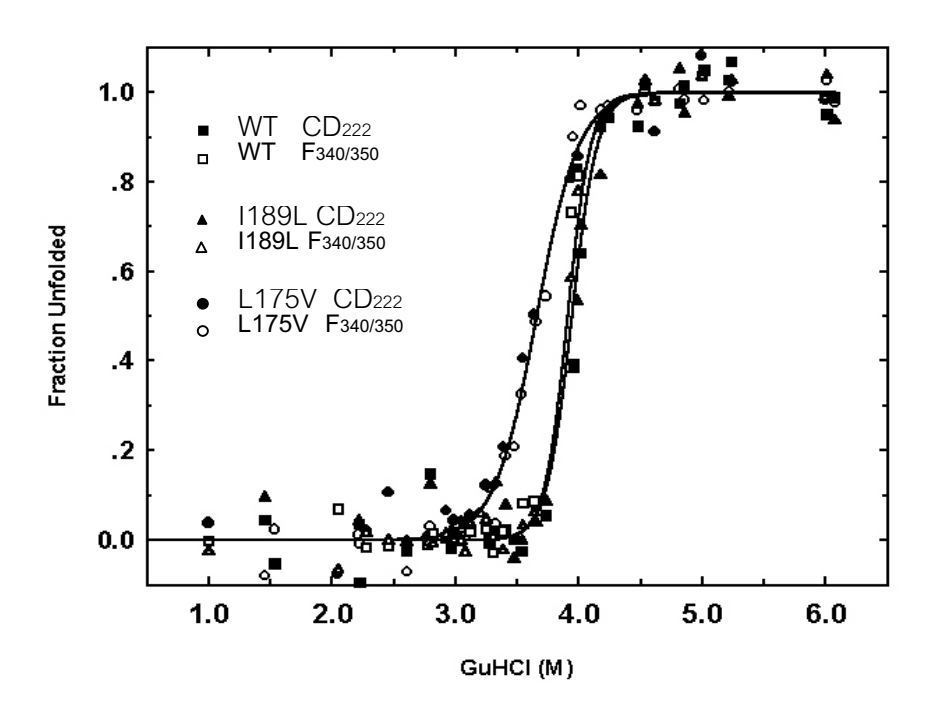


**Figure 28**: Unfolding curves of the block I mutants showing LO175V, I189L and their R203Q template.

Toxins	[GuHCl] <sup>50%</sup>	m	$\Delta G^{o}_{U,W}$	$\Delta\Delta G^{o}_{U,W}$
	(M)	(cal/mol <sup>·</sup> M)	(kcal/mol)	(kcal/mol)
R203Q	3.92	5890	23.09	0.00
L175V	3.66	3445	12.61	-10.48
I189L	3.94	5774	22.75	-0.34

Table 2: Steady state parameters derived from unfolding experiment of L175V, I189L and T203Q

According the calculated unfolding free energy, the native structure of L175V mutant is destabilized by 10.48 kcal/mol. This destabilization is very significant when compared to unfolding free energy of R203Q template at 23.09 kcal/mol. Since our analysis for stabilizing interactions in the three dimensional structure of domain I showed only the closed packing of hydrophobic cluster along the central helix-5, the destabilizing effect could be due to an interference on the hydrophobic core packing of this mutant.

However, the characterized unfolding free energy of I189L mutant remains unchanged. We have analyzed the mutational effect using a contact sphere around I189L and L175V. The model revealed that a substitution of L175 with V has generated a large cavity while a substitution of I189 with L has no significant change within the closed packing. This observation is also found in several cases of protein folding study. Here we have confirm the significant role of specific hydrophobic residues of the conserved block I on folding and stability of the molecular structure of the native toxin.

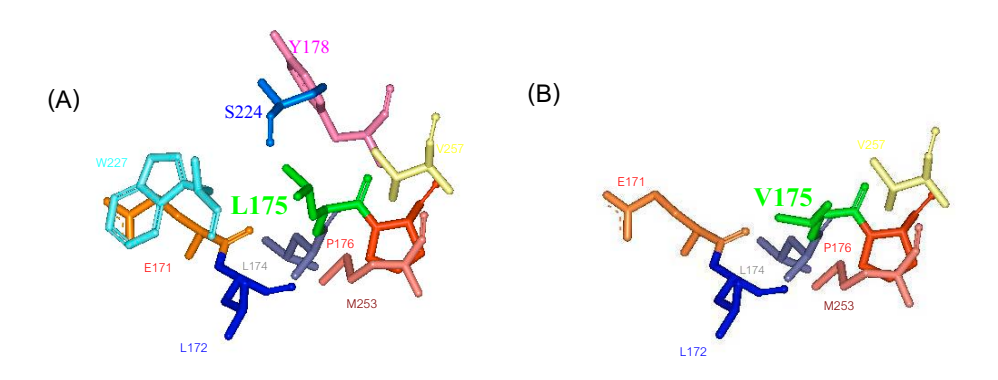


Figure 29: Molecular contact within a sphere of 5 A radius around the L175 (A) and V175 (B)

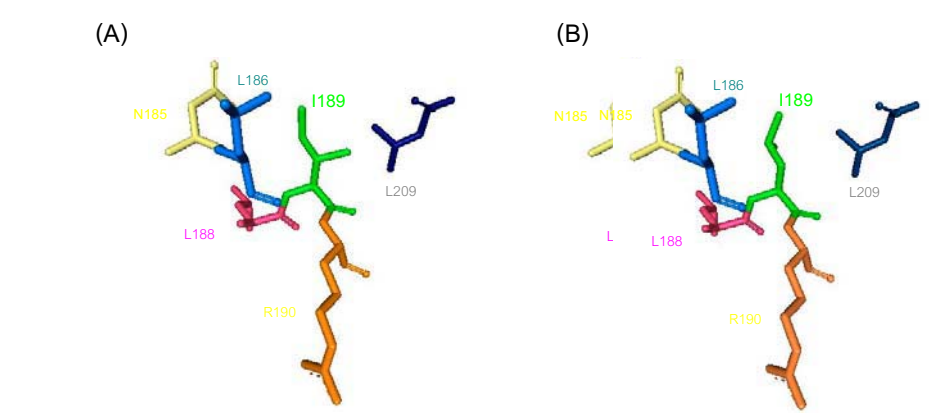


Figure 30: Molecular contact within a sphere of 5 A radius around the I189 (A) and L189 (B)

We have continued the characterization of these two mutants, L175V and I189L by an analysis of unfolding kinetics. Both mutants have demonstrated an exponential decay of the fluorescence intensity similar to their R203Q template (Figure 31-32).

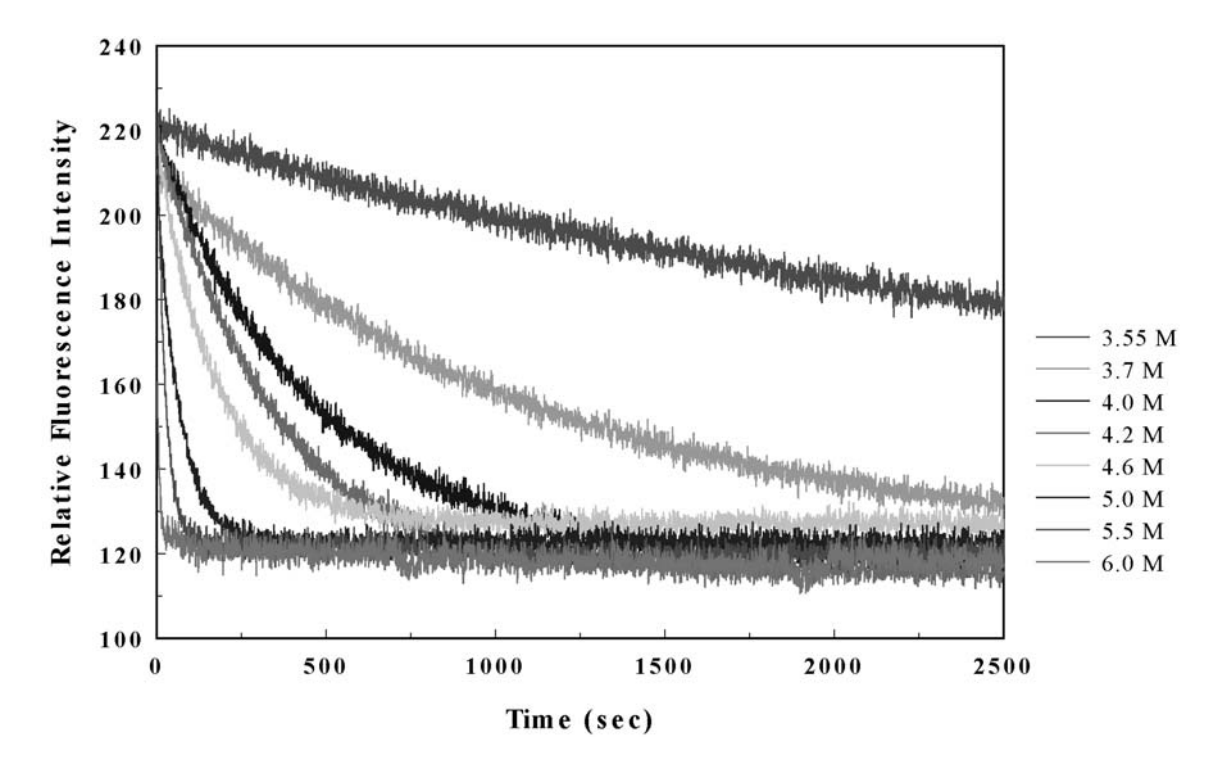


Figure 31: Analysis of unfolding kinetics of L175V mutant

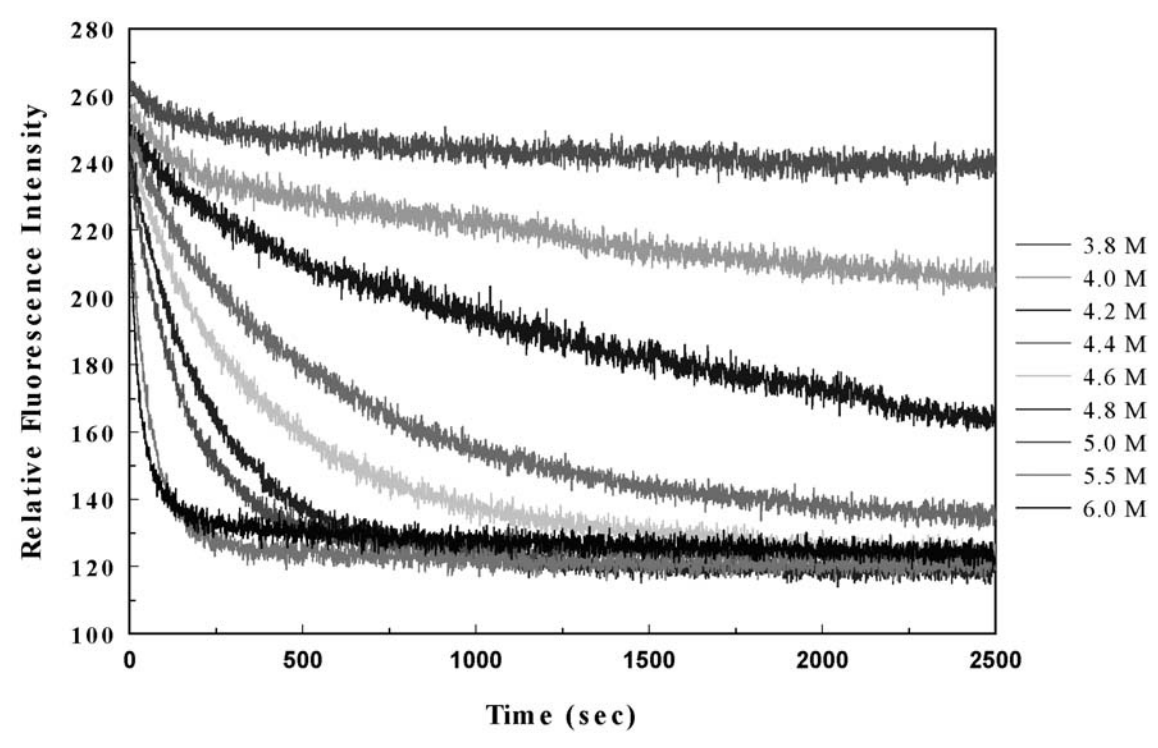


Figure 32: Analysis of unfolding kinetics of I189L mutant

Our calculation for the unfolding rate constant (Figure 33) ) and activation energy has revealed a similar value for both mutants(Table 3). It means that the introduced mutation on both positions has no effect on the kinetics or mechanism of the protein during an unfolding process. A combined data of unfolding free energy and activation energy was then used to sketch an energy profile of unfolding for each mutant (Figure 34). This energy profile can graphically demonstrate the mutational effect of L175V and I189L. It shows that the native state of L175V is destabilized by 10.4 kcal/mol relative to I189L and the R203Q template. The map also shows that the activation energy used to overcome the transitional barrier of the two mutants remain unchanged.

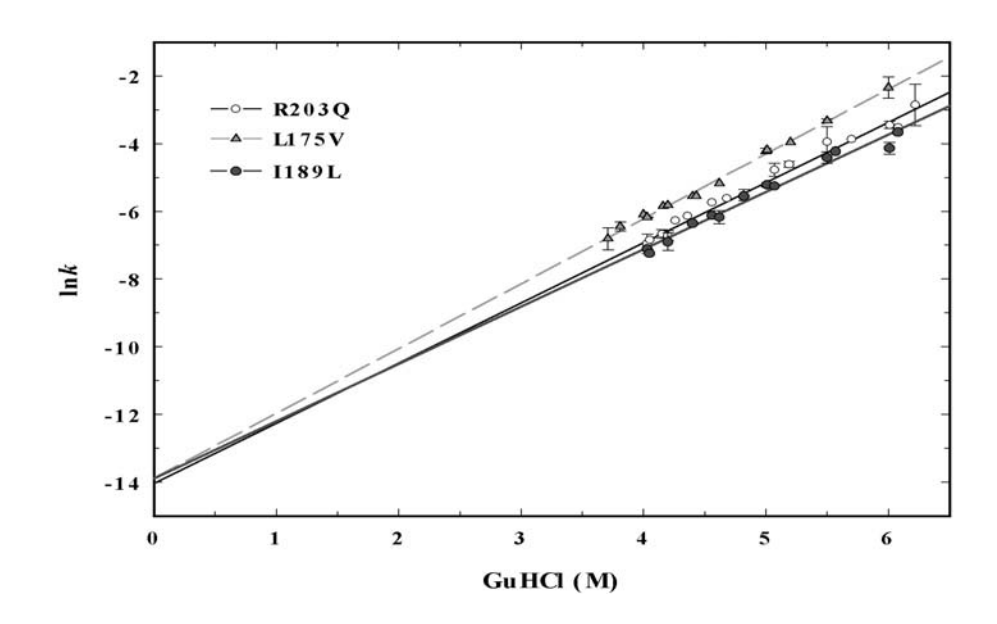


Figure 33: Determination of the unfolding rate constant of L175V and I189L

Toxins	$\ln k^{\circ}_{\mathrm{U,W}} \pm \mathrm{SEM}^{/1}$	$k^{o}_{U,W} \pm SEM$ (×10 <sup>-7</sup> s <sup>-1</sup> ) <sup>/2</sup>	Ea° <sub>U,W</sub> ± SEM (kcal/mol) /3	$\Delta E a^{\circ}_{U,W} \pm SEM$ (kcal/mol) /5
R203Q	$-13.94 \pm 0.09$	$8.90 \pm 0.85$	$25.71 \pm 0.06$	
L175V	$-14.03 \pm 0.36$	$9.06 \pm 3.01$	$25.76 \pm 0.21$	$+0.06 \pm 0.18$
I189L	$-13.80 \pm 0.30$	$10.99 \pm 2.81$	$25.62 \pm 0.17$	$-0.08 \pm 0.23$

**Table3**: Kinetics parameters from the unfolding of L175V and I189L in comparison with the R203Q template

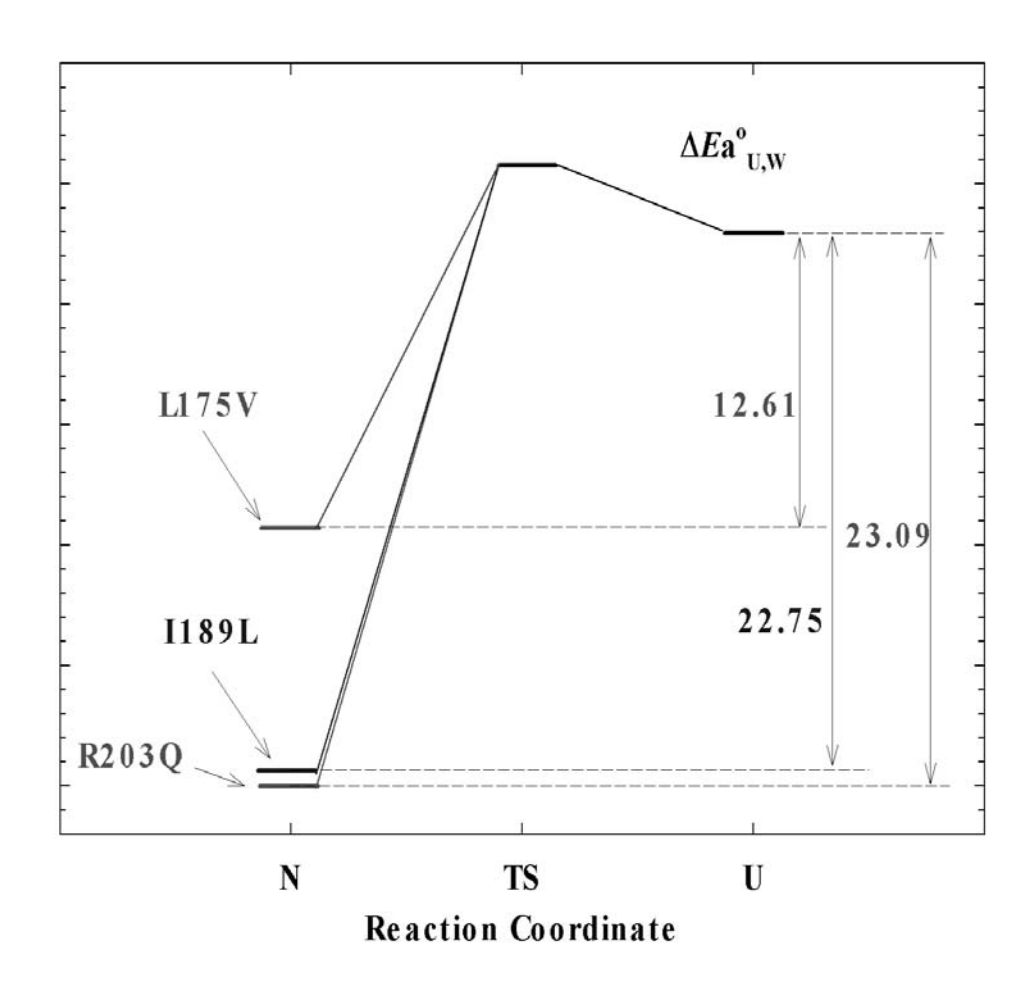


Figure 34: Energy map of protein unfolding constructed from a combined data from steady state and kinetics experiment

## 4.2. Roles of Hydrogen Bonding

A number of mutant toxins were constructed to investigate the role of identified hydrogen bonding provided by the residues of conserved sequence blocks. These mutants are R190, D191 (Block 1), Y267F, T285V, H466Y (Block 3), D470N, K487A, R627A and E629Q (Block 5), They were successfully constructed by PCR-based site-directed mutagenesis using R203Q as a template.

Biochemical characterization of these mutants showed that only H466Y, D470N and E629Q are soluble in the alkali carbonate buffer pH.9. The other expressed protein products of R190A, D191N, Y267F, T285V, K487A and R627A were found to be insoluble in the same buffer condition. Further processing of the130-kDa soluble protoxins by trypsin gave an expected active toxin molecule of 65 kDa for H466Y and D470N but gave no stable product for E629Q mutant. This is suggesting that although E629Q was obtained as the soluble product but the mutant can not adopt a correct folding leading to a complete digestion by proteases.

In summary we have successfully obtained 9 mutant proteins from the template. Two of them (H466Y and D470N) is suggested to be in the native conformation based on solubility and the processing pattern. The other seven mutants (R190A, D191N, Y267F, T285V, K487A, R627A and E629Q) are likely to have lost their native folding. An analysis of the x-ray structure of wild type toxin had indicated stabilizing hydrogen bonds between those mutated residues with other residues nearby. The criterion used for defining these hydrogen bonds is an existing of the hydrogen donor (D) and acceptor (A) with in the distance ranging around 2.5-3.3 angstrom apart. The Angle between D-H-A is also set below 90 degree.

The critical role of hydrogen bond revealed in these mutants can be discusses as a crucial stabilization required for the polypeptide chain to adopt the correct folding of the native toxin. These identified hydrogen bonds are listed in Table 4 and demonstrated in Figure 34-41. One would see that a majority of the eliminated hydrogen bond has a critical role for the protein to adopt the native folding, while a few of them do not show any effect in biochemical property. If we analyzed the position of amino acids that interact with our mutated residues, we can classify them into two groups. One is an amino acid located far away in sequence but come closer to the mutated residue in space. This kind of interaction provides stabilization for the tertiary structure of protein. The other group is a neighboring amino acid located nearby in the sequence and in space. Our result suggest that an elimination of the interaction contributing in tertiary structure stabilization will obstruct the

protein to adopt the correct folding as we saw in R190A, D191N, Y267F, T285V, K487A, R627A and E629Q.

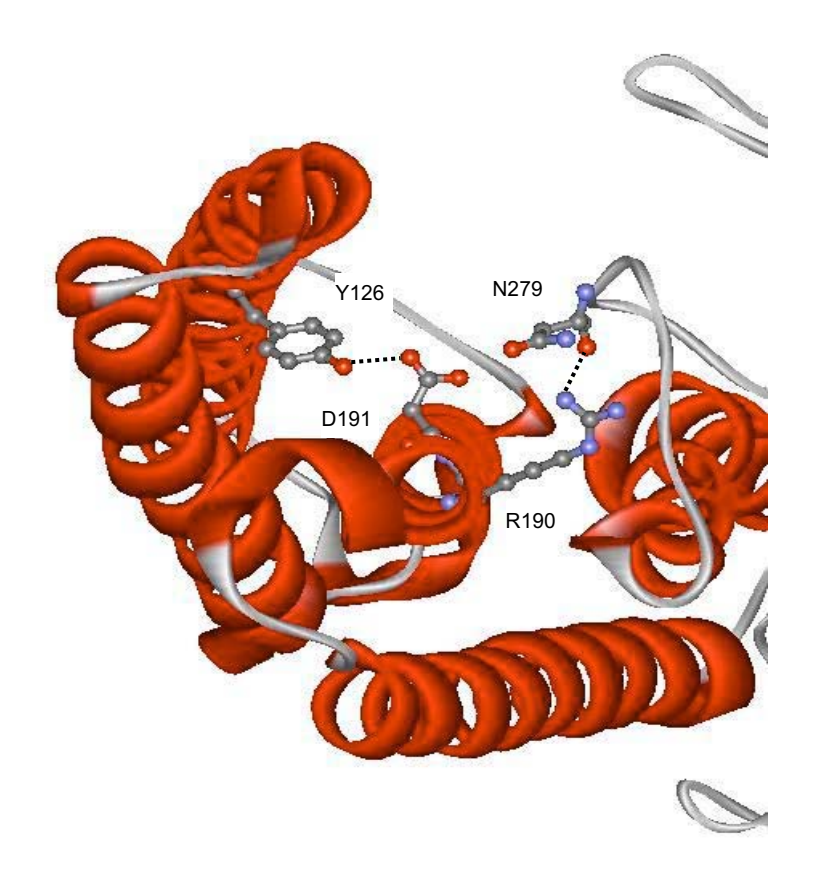


**Figure 34**: X-ray structure of the Cry4B toxin showing hydrogen bonding of R190 and D191

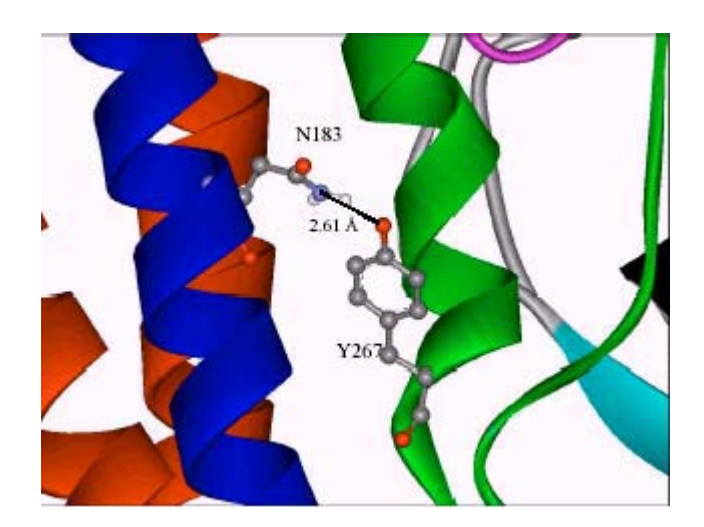


Figure 35: X-ray structure of the Cry4B toxin showing hydrogen bonding of Y269

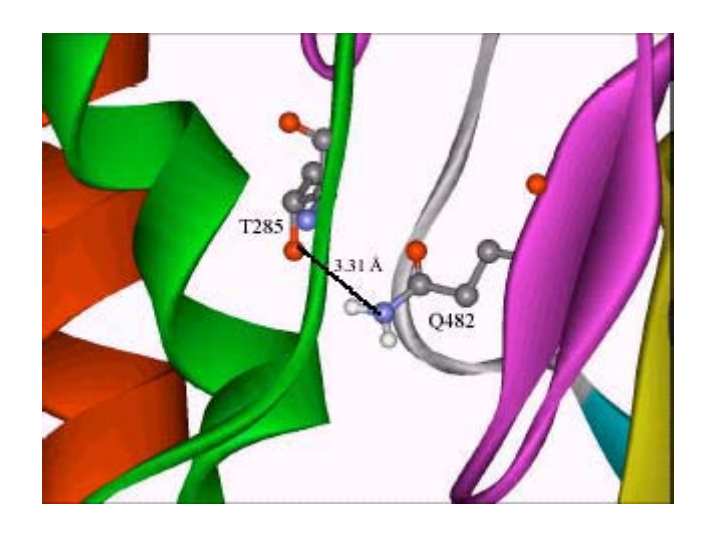


Figure 36: X-ray structure of the Cry4B toxin showing hydrogen bonding of T285

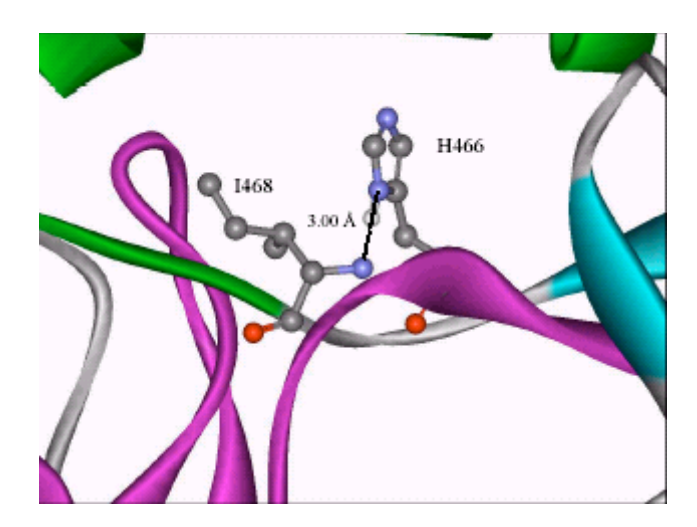


Figure 37: X-ray structure of the Cry4B toxin showing hydrogen bonding of H466

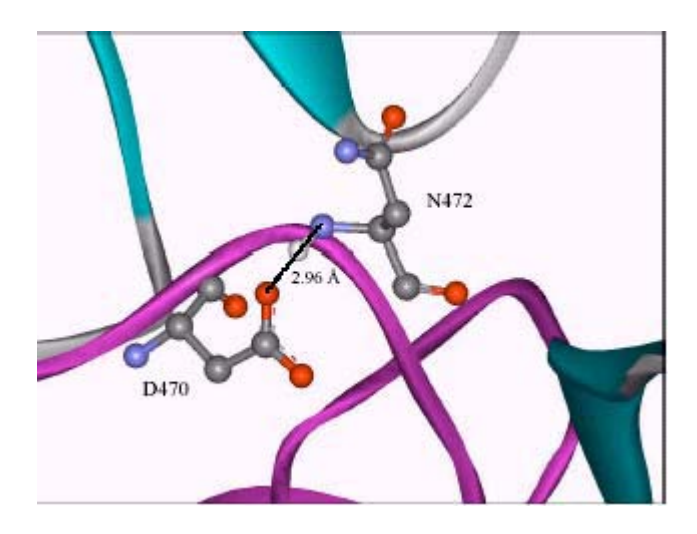


Figure 38: X-ray structure of the Cry4B toxin showing hydrogen bonding of D470

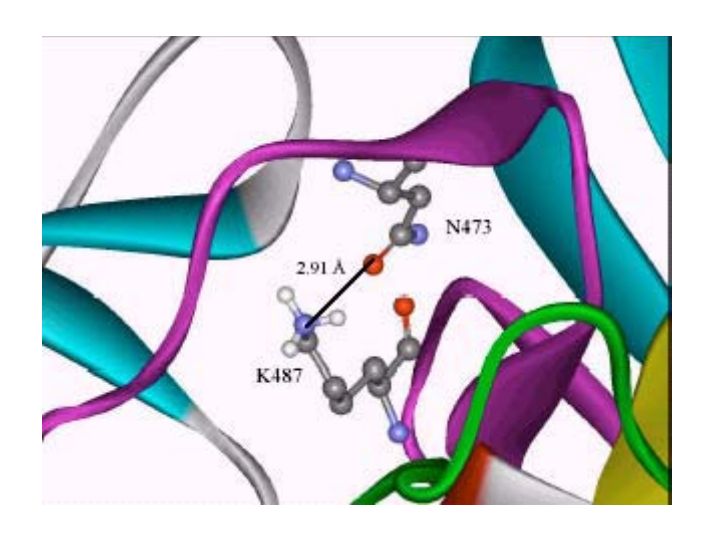


Figure 39: X-ray structure of the Cry4B toxin showing hydrogen bonding of K187



Figure 40: X-ray structure of the Cry4B toxin showing hydrogen bonding of R627

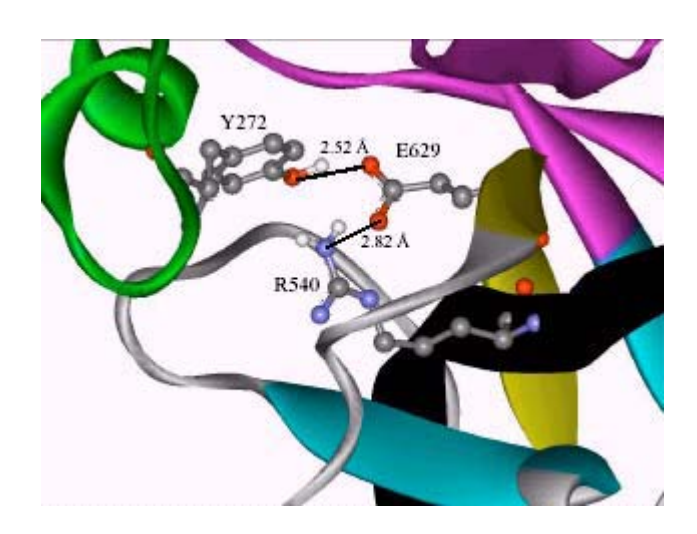


Figure 41: X-ray structure of the Cry4B toxin showing hydrogen bonding of E629

Block	Mutation	Type of	Interaction	Bond	Correct
		interaction	removed	distance A	folding
1	R190A	H-bond	R190 - N279	2.89	No
1	D191A	H-bond	D191 - Y126	2.79	No
3	Y267F	H-bond	Y267 - N183	2.61	No
3	T285V	H-bond	T285 - Q482	3.31	No
3	H466Y	H-bond	H466 - I468	3.00	Yes
3	D470N	H-bond	D470 - N472	2.98	Yes
3	K487A	H-bond	K487 - N473	2.91	No
5	R627A	H-bond	R627 - Y272	3.12	No
5	E629Q	H-bond	E629 - Y272	2.52	No
		H-bond	E629 - R627	2.73	

Table 4: A list of mutants with hydrogen bond eliminated from each conserved block

For the soluble H466Y and D470N mutants which is though to be in the correct native folding, further analysis by an unfolding experiment was then employed to assess for their molecular stability compared to the template. The results showed that their unfolding curves and the calculated unfolding free energy are very much closed to their template toxin (Table 5). This is a confirmation that mutation at the position H466Y and D470N does not have any affect on both structural folding and molecular stability of the toxin.

	[GuHCl] <sup>50%</sup> (M) <u>+</u> SD	(kcal.mol <sup>-1</sup> .M <sup>-1</sup> ) <u>+</u> SD	$\Delta G^{o}_{U, W}$ (kcal.mol <sup>-1</sup> ) $\pm SD$	ΔΔG° <sub>U, W</sub> (kcal.mol <sup>-1</sup> )
R203Q (template)	3,81 <u>+</u> 0,00	6.22 <u>+</u> 0.04	23.72 ± 0.17	0.00
H466Y	3.80 ± 0.02	5.62 ± 0.33	21.39 <u>+</u> 1.36	-2.33
D470N	3.74 ± 0.04	6.25 <u>+</u> 0.24	23.38 ± 1.15	-0.34

Table 5: Steady state parameters and unfolding free energy of H466Y and D470N mutants

## 4.3. Role of Electrostatic interaction

We have designed and constructed more mutants to investigate the role of selected salt bridge provided by residues of the conserved sequence blocks. These mutants are R251A and D259N (Block 2). These mutants were successfully constructed by PCR and characterized for their biochemical property. We have found that the two mutants can be expressed at a comparable level to that of the R203Q template. However the expressed D259N is found insoluble in the alkali carbonate buffer. The drastic change of toxin solubility has suggested that the expressed D259N mutant could not adopt the native conformation (Table 6).

However the expressed R251A was obtained as a soluble protein and can be processed to the 65-kDa active form. A possible explanation is based on the different nature between both salt bridges as identified from the x-ray structure of toxin. We found that the first electrostatic interaction or salt-bridge formed between R251 and neighboring D248 residue can help stabilizes the local folding of protein secondary structure (Figure 42). But the other interaction between D259 and R289 help stabilize protein tertiary structure (Figure 43). It is likely that an elimination of the interaction that stabilizes tertiary structure has led to a failure in adopting the native folding.

Block	Mutation	Type of	Interaction	Bond	Correct
		interaction	removed	distance A	folding
2	R251A	Salt bridge	R251 - D248	2.89	Yes
2	D259N	Salt bridge	D259 - R289	2.78	No

Table 6: A list of mutants with salt bridges eliminated

We have continued to analyze the soluble mutant toxin, R251A by an unfolding experiment. After a construction of unfolding curve and fitting the data to the two-state transition model, it was found that R251A give an identical unfolding curve and very similar unfolding free energy to the R203Q template (Table 7). This result means that a perturbation on the electrostatic interaction between R251 - D248 has no effect on structural folding and molecular stability of the toxin.

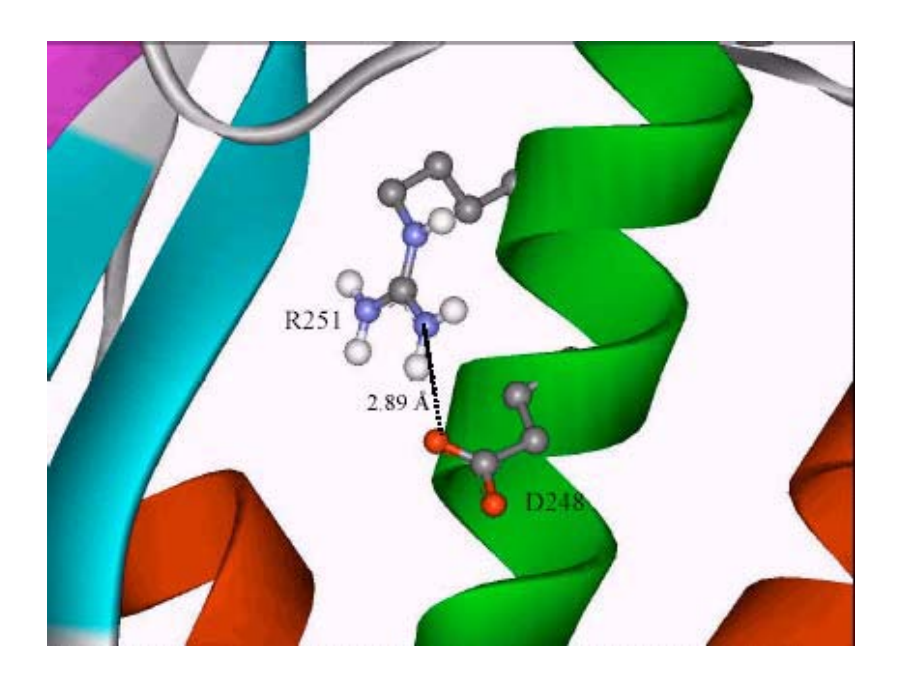


**Figure 42**: X-ray structure of the Cry4B toxin showing an electrostatic interaction formed between R251 and D248

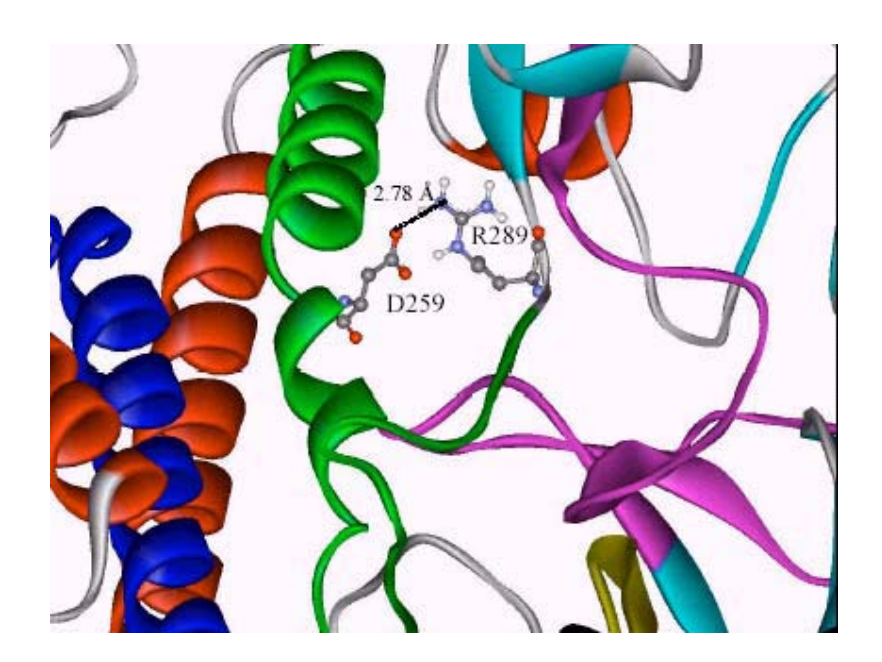


Figure 43: X-ray structure of the Cry4B toxin showing an electrostatic interaction formed between D259 and R289

	[GuHCl] <sup>50%</sup> (M) ± SD	(kcal.mol <sup>-1</sup> .M <sup>-1</sup> ) ± SD	$\Delta G^{\circ}_{U, W}$ (kcal.mol <sup>-1</sup> ) $\pm SD$	$\Delta\Delta G^{\circ}_{U,W}$ (kcal.mol <sup>-1</sup> )
R203Q (template)	3.81 <u>+</u> 0.00	6.22 ± 0.04	23.72 ± 0.17	0.00
R251A	3.80 <u>+</u> 0.03	6.58 ± 0.00	24.98 ± 0.18	+1.26

Table 7: Steady state parameters and unfolding free energy of R251A

# 5. Characterization of Larvicidal Activity

According to all the generated mutants, they were characterized for the basic biochemical property in terms of expression level, solubility, proteolytic processing pattern. Here we also examined the biological activity of these mutant toxins. After feeding the 2-day old *A. aegypti* larvae with the cells expressing for the toxin, the mortality rate of larvae was then reported. We found that the mutants adopting the native-like structure (R203Q, L175V, I189L, R251A, H466Y and D470N) showed their toxicity similar to the wild type around 80-90%. On the contrary, those mutants which are insoluble or sensitive to a complete digestion by trypsin showed a marked drop of their activity against the larvae. These results confirm that the biological functionality is closely related to the correct structural folding of the toxins.

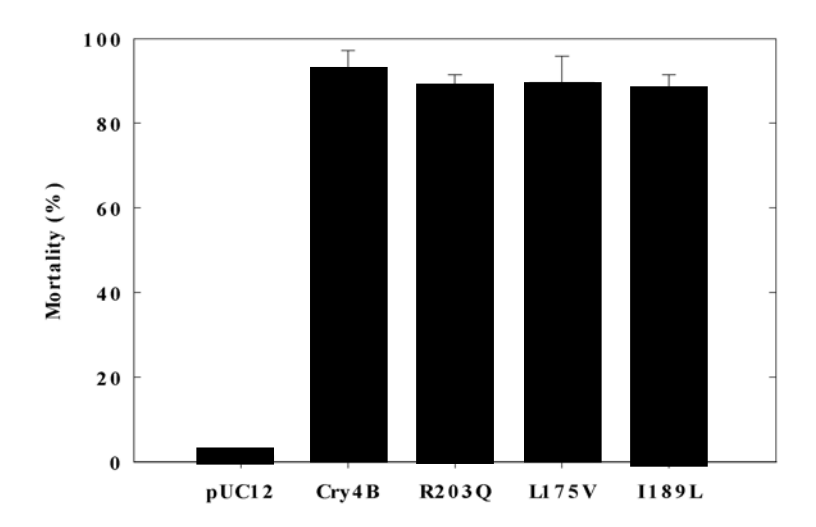


Figure 44: Larvicidal activity of wild type, R203Q template and mutants

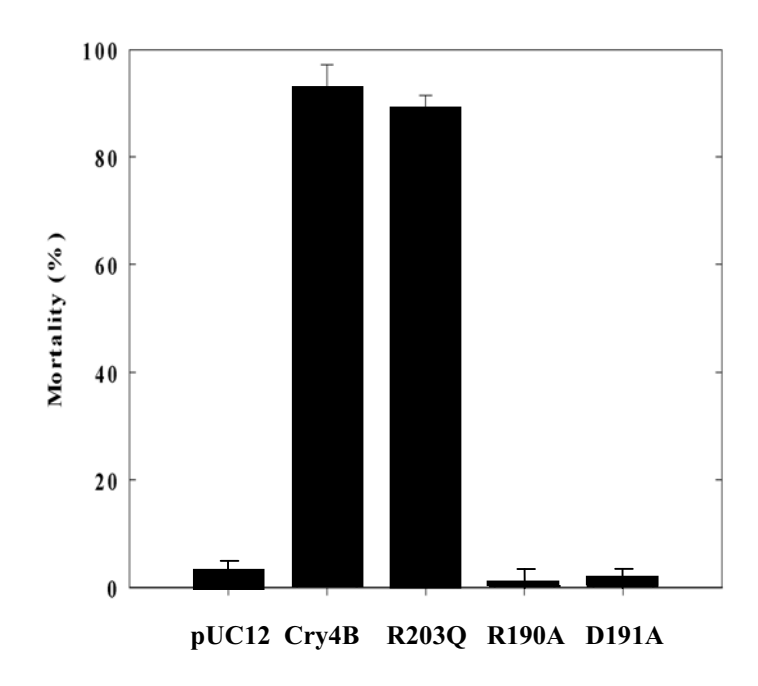


Figure 45: Larvicidal activity of wild type, R203Q template and mutants

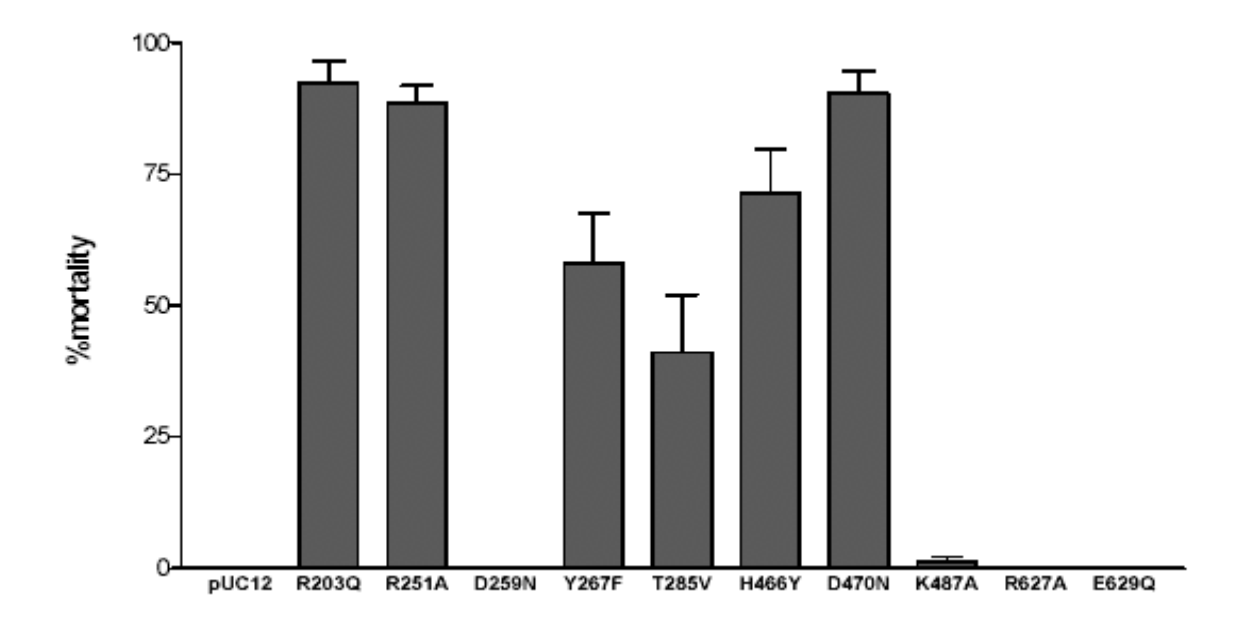


Figure 46: Larvicidal activity of R203Q template and mutants

# **Concluding Remarks**

- 1. Characterization of protein unfolding for wild type Cry4B has revealed an unfolding free energy of 17.86 kcal/mol and activation energy of 25.77 kcal/mol, respectively.
- 2. A single chain R203Q mutant has demonstrated an enhanced stability with an unfolding free energy of 23.09 kcal/mol and activation energy of 25.71 kcal/mol.
- 3. The mutant plasmids, pL175V, pl189L, pR190A, pD191A, pR251A, pD259N, pY267F, pT285V, pH466Y, pD470N, pK487A, pR627A and pE629Q, were successfully constructed by PCR-based site directed mutagenesis using pR203Q as a template, and their nucleotide sequences were confirmed by automated DNA sequencing.
- 4. The expression levels of these mutant toxins are comparable to that of R203Q template.
- 5. Based toxin solubility and proteolytic processing pattern, L175V, I189L, R251A, H466Y and D470N mutant toxins were expressed in the native-like conformation while R190A, YD259N, Y267F, T285V, K487A and R627A could not adopt the correct folding due to losing of hydrogen bond and electrostatic interaction in the conserved blocks.
- 6. The chemical unfolding curves and unfolding free energy of the purified I189L, R251A, H466Y and D470N were found similar to that of R203Q template. However a perturbation of the hydrophobic packing inside the domain interior of L175V has led to a significant destabilization of molecular structure by 10.49 kcal/mol
- 7. Stabilizing hydrogen bond and electrostatic interaction that helps maintain protein tertiary structure is more important than those interactions within a secondary structure element.
- 8. Specific stabilizing interaction formed between the residues located on the five conserved blocks is highly critical for the correct folding of Cry4B.

.

### **REFERENCES**

- 1. Bychkova VE, Ptitsyn OB. Folding intermediates are involved in genetic diseases? FEBS Lett. 1995; 359(1):6-8.
- 2. Eigen M. Prionics or the kinetic basis of prion diseases. Biophys Chem. 1996; 63(1):A1-18. Review.
- 3. Booth DR, Sunde M, Bellotti V, Robinson CV, Hutchinson WL, Fraser PE, Hawkins PN, Dobson CM, Radford SE, Blake CC, Pepys MB. Instability, unfolding and aggregation of human lysozyme variants underlying amyloid fibrillogenesis. Nature. 1997; 385(6619):787-93.
- 4. Klibanov AM. Enzymatic catalysis in anhydrous organic solvents. Trends Biochem Sci. 1989; 14(4):141-4. Review.
- 5. Griebenow K, Klibanov AM. Can conformational changes be responsible for solvent and excipient effects on the catalytic behavior of subtilisin Carlsberg in organic solvents? Biotecnol. Bioeng. 1997; 53:351-362.
- 6. Levinthal C. Are there pathways for protein folding? J Chim Physique. 1968; 65:44-45.
- 7. Anfinsen CB, Haber E, Sela M, White FH. The kinetics of formation of native ribonuclease during oxidation of the reduced polypeptide chain. Proc Natl Acad Sci USA 1961; 47(9):1309-14.
- 8. Anfinsen CB. Principles that govern the folding of protein chains. Science. 1973; 181 (96):223-30.
- 9. Govindarajan S, Goldstein RA. On the thermodynamic hypothesis of protein folding. Proc Natl Acad Sci U S A. 1998; 95(10):5545-9.
- 10. Frauenfelder H, Sligar SG, Wolynes PG. The energy landscapes and motions of proteins. Science. 1991; 254(5038):1598-603.
- 11. Fersht AR.The sixth Datta Lecture. Protein folding and stability: the pathway of folding of barnase. FEBS Lett. 1993; 325(1-2):5-16. Review.
- 12. Chan HS. Kinetics of protein folding. Nature. 1995; 373:664-5.
- 13. Nolting B, Golbik R, Fersht AR. Submillisecond events in protein folding. Proc Natl Acad Sci U S A. 1995; 92(23):10668-72.
- 14. Nolting B, Golbik R, Neira JL, Soler-Gonzalez AS, Schreiber G, Fersht AR. The folding pathway of a protein at high resolution from microseconds to seconds. Proc Natl Acad Sci U S A. 1997; 94(3):826-30.
- 15. Eaton WA, Thompson PA, Chan CK, Hage SJ, Hofrichter J. Fast events in protein folding. Structure. 1996; 4(10):1133-9. Review.

- 16. Finkelstein AV. Protein structure: what is it possible to predict now? Curr Opin Struct Biol. 1997; 7(1):60-71. Review.
- 17. Ptitsyn OB. Protein evolution and protein folding: non-functional conserved residues and their probable role. Pac Symp Biocomput. 1999;:494-504.
- 18. Mirny L, Shakhnovich E. Evolutionary conservation of the folding nucleus. J Mol Biol. 2001; 308(2):123-9.
- 19. Itzhaki L, Otzen D, Fersht AR. The structure of the transition state for folding of chymotrypsin inhibitor 2 analyzed by protein engineering methods: evidence for a nucleation-condensation mechanism for protein folding. J. Mol. Biol. 1995; 254:260-288.
- 20. Lopez-Hernandez E. Serrano L. Structure of the transition state for folding of the 129 aa protein chey resembles that of a smaller protein, ci2. Fold. Des. 1996; 1:43-55.
- 21. Vilegas V, Martinez J, Avilez F, Serrano L. Structure of the transition state in the folding process of human procarboxypeptidase a2 activation domain. J. Mol. Biol. 1998; 283:1027-1036.
- 22. Lorch M, Mason J, Clarke A, Parker M. Effects of core mutations on the folding of a betasheet protein: implications for backbone organization in the i-state. Biochemistry 1999; 38:1377-1385.
- 23. Dill KA. Dominant forces in protein folding. Biochemistry 1990; 29:7133-55.
- 24. Richards FM, Lim WA. An analysis of packing in the protein folding problem. Quart Rev. Biophys. 1993; 26:423-98.
- 25. Grantcharova VP, Riddle DS, Santiago JV, Baker D. Important role of hydrogen bonds in the structurally polarized transition state for folding of the src SH3 domain. Nat Struct Biol. 1998; 5(8):714-20.
- 26. Kumar S, Nussinov R. Salt bridge stability in monomeric proteins. J Mol Biol. 1999; 293 (5):1241-55.
- 27. Kumar S, Ma B, Tsai CJ, Nussinov R. Electrostatic strengths of salt bridges in thermophilic and mesophilic glutamate dehydrogenase monomers. Proteins. 2000; 38(4):368-83.
- 28. Kumar S, Wolfson HJ, Nussinov R. Protein flexibility and electrostatic interactions. IBM J. RES. & DEV. 2001; 45(3/4):499-512.
- 29. Griko YV, Privalov PL. Calorimetric study of the heat and cold denaturation of beta-lactoglobulin. Biochemistry. 1992; 31(37):8810-5.
- 30. Cavagnero S, Debe DA, Zhou ZH, Adams MW, Chan SI. Kinetic role of electrostatic interactions in the unfolding of hyperthermophilic and mesophilic rubredoxins. Biochemistry. 1998; 37(10):3369-3376.

- 31. Hill RB, DeGrado WF. A polar, solvent-exposed residue can be essential for native protein structure. Structure Fold Des. 2000; 8(5):471-9.
- 32. Leung KW, Liaw YC, Chan SC, Lo HY, Musayev FN, Chen JZ, Fang HJ, Chen HM. Significance of local electrostatic interactions in staphylococcal nuclease studied by site-directed mutagenesis. J Biol Chem. 2001; 276(49):46039-45.
- 33. Pathaichindachote W. Folding and stability investigation of the activated *Bacillus thuringiensis* Cry4B toxin by site-directed mutagenesis at the conserved aspatic acid-191. [MSc. Thesis in Molecular Genetics and Genetic Engineering] Mahidol University, 2002.
- 34. Marqusee S, Sauer RT. Contributions of a hydrogen bond/salt bridge network to the stability of secondary and tertiary structure in lambda repressor. Protein Sci. 1994; 3(12):2217-25.
- 35. Pedone E, Cannio R, Saviano M, Rossi M, Bartolucci S. Prediction and experimental testing of Bacillus acidocaldarius thioredoxin stability. Biochem J. 1999; 339 (Pt 2):309-17.
- 36. Lin TY. G33D mutant thioredoxin primarily affects the kinetics of reaction with thioredoxin reductase. Probing the structure of the mutant protein. Biochemistry. 1999; 38(47):15508-13.
- 37. Blaber SI, Culajay JF, Khurana A, Blaber M. Reversible thermal denaturation of human FGF-1 induced by low concentrations of guanidine hydrochloride. Biophys J. 1999; 77(1):470-7.
- 38. Culajay JF, Blaber SI, Khurana A, Blaber M. Thermodynamic characterization of mutants of human fibroblast growth factor 1 with an increased physiological half-life. Biochemistry. 2000; 39(24):7153-8.
- 39. Hornby JA, Luo JK, Stevens JM, Wallace LA, Kaplan W, Armstrong RN, Dirr HW. Equilibrium folding of dimeric class mu glutathione transferases involves a stable monomeric intermediate. Biochemistry. 2000; 39(40):12336-44.
- 40. Guihard G, Laprade R, Schwartz JL. Unfolding affects insect cell permeabilization by *Bacillus thuringiensis* Cry1C toxin. Biochim Biophys Acta. 2001; 1515(2):110-9.
- 41. Sundd M, Iverson N, Ibarra-Molero B, Sanchez-Ruiz JM, Robertson AD. Electrostatic interactions in ubiquitin: stabilization of carboxylates by lysine amino groups. Biochemistry. 2002; 41(24):7586-96.
- 42. Shirley BA. Protein stability and folding, theory and practice. Humana Press Inc. 1995:177-190.
- 43. Beegle CC, Yamamoto T. History of *Bacillus thuringiensis* Berliner research and development. Can Entomol 1992; 124:587-616.
- 44. Schnepf E, Crickmore N, Van Rie J, Lereclus D, Baum J, Feitelson J et al. *Bacillus thuringiensis* and its pesticidal crystal proteins. Microbiol. Mol. Biol. Rev. 1998; 62:775-806.

- 45. Feitelson JS, Payne J, Kim L. *Bacillus thuringiensis*: insects and beyond. Bio/Technology 1992; 10:271–5.
- 46. Feitelson JS. The *Bacillus thuringiensis* family tree, *In* L. Kim (ed.), Advanced engineered pesticides. Marcel Dekker, Inc., New York, N.Y. 1993;63-71.
- 47. Von Tersch MA, Slatin SL, Kulesza CA, English LH. Membrane-permeabilizing activities of *Bacillus thuringiensis* coleopteran-active toxin CrylllB2 and CrylllB2 domain I peptide. Appl Environ Microbiol 1994;60(10):3711-7.
- 48. Chen XJ, Curtiss A, Alcantara E, Dean DH. Mutations in domain I of *Bacillus thuringiensis* delta-endotoxin CrylAb reduce the irreversible binding of toxin to *Manduca sexta* brush border membrane vesicles. J Biol Chem 1995; 270(11):6412-9.
- 49. Dean DH, Rajamohan F, Lee MK, Wu SJ, Chen XJ, Alcantara E, Hussain SR. Probing the mechanism of action of *Bacillus thuringiensis* insecticidal proteins by site-directed mutagenesis. Gene 1996; 179(1):111-7.
- 50. Gazit E, La Rocca P, Sansom MS, Shai Y. The structure and organization within the membrane of the helices composing the pore-forming domain of *Bacillus thuringiensis* delta-endotoxin are consistent with an "umbrella-like" structure of the pore. Proc Natl Acad Sci USA 1998; 95(21):12289-94.
- 51. Alcantara EP, Alzate O, Lee MK, Curtiss A, Dean DH. Role of u-helix seven of *Bacillus thuringiensis* Cry1Ab \( \frac{1}{2}\)-endotoxin in membrane insertion, structural stability, and ion channel activity. Biochemistry 2001; 40(8):2540-2547.
- 52. Widner WR, Whiteley HR. Location of the dipteran specificity region in a lepidipterandipteran crystal protein from *Bacillus thuringiensis*. J Bacteriol 1990; 172(6):2826-32.
- 53. Lu H, Rajamohan F, Dean DH. Identification of amino acid residues of *Bacillus thuringiensis* delta-endotoxin CrylAa associated with membrane binding and toxicity to *Bombyx mori*. J Bacteriol 1994; 176(17):5554-9.
- 54. Smith GP, Ellar DJ. Mutagenesis of two surface-exposed loops of the *Bacillus thuringiensis* CrylC delta-endotoxin affects insecticidal specificity. Biochem J 1994; 302:611-6.
- 55. Rajamohan F, Alcantara E, Lee MK, Chen XJ, Curtiss A, Dean DH. Single amino acid changes in domain II of *Bacillus thuringiensis* CrylAb delta-endotoxin affect irreversible binding to *Manduca sexta* midgut membrane vesicles. J Bacteriol 1995; 177(9):2276-82.
- 56. Rajamohan F, Cotrill JA, Gould F, Dean DH. Role of domain II, loop 2 residues of *Bacillus thuringiensis* CrylAb delta-endotoxin in reversible and irreversible binding to *Manduca sexta* and *Heliothis virescens*. J Biol Chem 1996; 271(5):2390-6.

- 57. Rajamohan F, Alzate O, Cotrill JA, Curtiss A, Dean DH. Protein engineering of *Bacillus thuringiensis* delta-endotoxin: mutations at domain II of CrylAb enhance receptor affinity and toxicity toward gypsy moth larvae. Proc Natl Acad Sci U S A 1996; 93(25):14338-43.
- 58. Rajamohan F, Hussain SRA, Cotrill JA, Gould F, Dean DH. Mutations at domain II, loop 3, of *Bacillus thuringiensis* CrylAa and CrylAb delta-endotoxins suggest loop 3 is involved in initial binding to lepidopteran midguts. J Biol Chem 1996; 271(41):25220-6.
- 59. Lee MK, You TH, Curtiss A, Dean DH. Involvement of two amino acid residues in the loop region of *Bacillus thuringiensis* Cry1Ab toxin in toxicity and binding to *Lymantria dispar*. Biochem Biophys Res Commun 1996; 229(1):139-46.
- 60. Wu SJ, Dean DH. Functional significance of loops in the receptor binding domain of *Bacillus thuringiensis* CryIIIA delta-endotoxin. J Mol Biol 1996; 255(4):628-40.
- 61. Smedley DP, Ellar DJ. Mutagenesis of three surface-exposed loops of a *Bacillus thuringiensis* insecticidal toxin reveals residues important for toxicity, receptor recognition and possibly membrane insertion. Microbiology 1996; 142(Pt 7):1617-24.
- 62. Lee MK, Young BA, Dean DH. Domain III exchanges of *Bacillus thuringiensis* CrylA toxins affect binding to different gypsy moth midgut receptors. Biochem Biophys Res Commun 1995; 216(1):306-12.
- 63. de Maagd RA, Kwa MS, van der Klei H, Yamamoto T, Schipper B, Vlak JM *et al.* Domain III substitution in *Bacillus thuringiensis* delta-endotoxin CrylA(b) results in superior toxicity for *Spodoptera exigua* and altered membrane protein recognition. Appl Environ Microbiol 1996; 62 (5):1537-43.
- 64. de Maagd RA, Bakker PL, Masson L, Adang MJ, Sangadala S, Stiekema W, Bosch D. Domain III of the *Bacillus thuringiensis* delta-endotoxin Cry1Ac is involved in binding to *Manduca sexta* brush border membranes and to its purified aminopeptidase N. Mol Microbiol 1999; 31(2):463-71.
- 65. Schwartz JL, Potvin L, Chen XJ, Brousseau R, Laprade R, Dean DH. Single-site mutations in the conserved alternating-arginine region affect ionic channels formed by CrylAa, a *Bacillus thuringiensis* toxin. Appl Environ Microbiol 1997; 63(10):3978-3984.
- 66. Knowles BH, Dow JAT. The crystal \( \frac{1}{2}\)-endotoxins of *Bacillus thuringiensis*: Model for their mechanism of action on the insect gut. Bioassays 1993; 15:469-76.
- 67. Knowles BH. Mechanism of action of *Bacillus thuringiensis* insecticidal <sup>1</sup>-endotoxins. Adv Insect Physiol. 1994; 24:275-308.
- 68. Rajamohan F, Lee MK, Dean DH. *Bacillus thuringiensis* insecticidal proteins: molecular mode of action. Prog Nucleic Acid Res Mol Biol. 1998; 60:1-27. Review.

- 69. Schnepf HE, Tomczak K, Ortega JP, Whiteley HR. Specificity-determining regions of a lediopteran-specific insecticidal protein produced by *Bacillus thuringiensis*. J Bio Chem. 1990; 265(34):20923-20930.
- 70. Li J, Carroll J, Ellar DJ. Crystal structure of insecticidal delta-endotoxin from *Bacillus* thuringiensis at 2.5 ន resolution. Nature 1991; 353(6347):815-21.
- 71. Hofte H, Whiteley HR. Insecticidal crystal proteins of *Bacillus thuringiensis*. Microbiol Rev 1989; 53(2):242-55.
- 72. Thompson MA, Schnepf HE, Feitelson JS. Structure, function, and engineering of *Bacillus thuringiensis* toxins, In J. K. Setlow (ed.), Genetic engineering: principles and methods. Plenum Press, New York, N.Y. 1995; 17:99-117.
- 73. Angsuthanasombat C, Crickmore N, Ellar DJ. Cytotoxicity of a cloned *Bacillus thuringiensis* subsp. *israelensis* CrylVB toxins to an *Aedes aegypti* cell line. FEMS Microbiol Letts 1991; 83:273-76.
- 74. Angsuthanasombat C, Crickmore N, Ellar DJ. Effects on toxicity of eliminating a cleavage site in a predicted interhelical loop in *Bacillus thuringiensis* CryIVB <sup>↑</sup>-endotoxin. FEMS Microbiol Letts 1993; 111:255-62.
- 75. Bourchookarn A, Site-directed mutagenesis and stability characterization of selected residues in Cry4B domainI. [MSc. Thesis in Molecular Genetics and Genetic Engineering] Mahidol University, 2003.
- 76. Boonserm P, Structure-function studies of the *Bacillus thuringiensis* subsp. *israelensis* mosquitocidal toxins. [Ph.D. Thesis in Biochemistry] University of Cambridge UK, 2002.
- 77. Lungchukiet P. Mutagenesis investigation of the arginine residue on helix 5 of the *Bacillus thuringiensis* Cry4B toxin. [MSc. Thesis in Molecular Genetics and Genetic Engineering] Mahidol University, 2000.
- 78. Angsuthanasombat C, Chungjatupornchai W, Kertbundit et al. Cloning and expression of 130-kDa mosquito-larvicidal delta-endotoxin gene of *Bacillus thuringiensis* var. *israelensis* in *Escherichia coli*. Mol Gen Genet 1987; 208(3):384-9.
- 79. Del Sal G, Manfioletti G, Schneider C. The CTAB-DNA precipitation method: a common mini scale preparation of template DNA from phagemids, phages or plasmids suitable for sequencing. Biotechniques 1989; 7(5): 514-20.
- 80. Sambrook J, Fritsch EF, Maniatis T. Molecular cloning: A Laboratory Manual. 2nd ed. Cold Spring Harbor, NY: Cold Spring Harbor Laboratory Press;1989.
- 81. Sanger F, Nicklen S, Coulson AR. DNA sequencing with chain terminating inhibitors. Proc Natl Acad Sci USA 1977; 74:5463-7.

- 82. Smith LM, Sanders JZ, Kaiser RJ, Hughes P, Dodd C, Hood LE, et al. Fluorescence detection in automated DNA sequence analysis. Nature 1986; 321:674-6.
- 83. Chen M, Christen P. Removal of chromosomal DNA by Mg2+ in the lysis buffer: an improved lysis protocol for preparing *Escherichia coli* whole cell lysate for sodium dodecyl sulfate-polyacrylamide gel electrophoresis. Anal Biochem 1997; 246(2):263-4.
- 84. Laemmli UK, Molbert E, Shown M, Kellenberger E. Form-determining function of the genes required for the assembly of the head of bacteriophage T4. J Mol Biol 1970; 49(1):99-113.
- 85. Bradford MM. A rapid and sensitive method for the quantitation for microgram quantities of protein utilizing the principle of protein-dye binding. Anal Biochem 1976; 72:248-54.
- 86. Waddell, WJ. A simple UV spectrophotometric method for the determination of protein. J Lab Clin Med 1956; 48:311-314.
- 87. Nozaki Y. The preparation of guanidine hydrochloride. Methods Enzymol. 1972; 26:43-50.
- 88. Kawahara K, Tanford C. Viscosity and density of aqueous solutions of urea and guanidine hydrochloride. J Biol Chem. 1966; 241(13):3228-32.
- 89. Nath U, Udgaonkar JB. Folding of tryptophan mutants of barstar: evidence for an initial hydrophobic collapse on the folding pathway. Biochemistry. 1997; 36(28):8602-10.
- 90. Ibarra-Molero B, Sanchez-Ruiz JM. A model-independent, nonlinear extrapolation procedure for the characterization of protein folding energetics from solvent-denaturation data. Biochemistry. 1996; 35(47):14689-702.
- 91. Soulages JL. Chemical denaturation: potential impact of undetected intermediates in the free energy of unfolding and *m*-values obtained from a two-state assumption. Biophys J. 1998; 75(1):484-92.

# **Outputs from the Project**

# 1. Publications in an international journal

- 1.1 Krittanai, C., Bourchookarn, A., Pathaichindachote, W. and Panyim, S. (2003)
  Mutation of the hydrophobic residues on helix 0.5 of the *Bacillus thuringiensis*Cry4B affects structural stability. *Protein & Pept. Letters* 4: 361-368.
- 1.2 Krittanai, C., Sangcharoen, A. and Taepanunt, W. Stabilizing interaction provided by the five conserved blocks of Cry4B toxin are critical for the correct folding. In Preparation.

# 2. Presentations in an international symposium

- 2.1 Krittanai, C., Pathaichindachote, W., Bourchookarn, A., Angsuthanasombat, C. and Panyim, S. Investigation of Denaturation Curves for Cry 4B Delta-Endotoxin The 46<sup>th</sup> Annual Meeting of Biophysical Society, San Francisco, USA., 23-27 February 2002.
- 2.2 Ounjai, P., Boonserm, P., Krittanai, C., Katzenmeier, G., Panyim, S. and Angsuthanasombat, C. Mutagenic Analysis of a Highly Conserved Arginine in an Alternating Arginine Region within Domain III of the Bacillus thuringiensis Cry4B Toxin The 46thAnnual Meeting of Biophysical Society, San Francisco, USA., 23-27 February 2002.
- 2.3 Krittanai, C., Bourchookarn, A. and Sangcharoen, A. Investigation of the Bacillus thuringiensis Cry4B Protein Unfolding by Circular Dichroism and Fluorescence Spectroscopy The Inaugural Austral-Asian Biospectroscopy Conference. Suranaree University of Technology, Thailand, February 3-7, 2003.
- 2.4 Krittanai, C., Bourchookarn, A., Sangcharoen, A. and Panyim, S. Mutation of the Hydrophobic Residues in the Interior of the Bacillus thuringiensis Cry4B Domain I Affects Structural Folding and Stability The 5<sup>th</sup> European Symposium of the Protein Society, Florence, Italy, March 29 April 2, 2003

# 3. Presentation in national symposium

3.1 Characterization of Protein Unfolding for *Bacillus thuringiensis* Cry4B Toxin by Stoppedflow Circular Dichroism Spectroscopy

In Protein Network Symposium on Protein Structure and Molecular Enzymology August 29-30, 2002, Faculty of Science, Mahidol University

3.2 Elimination of an Internal Cleavage Improved Structural Stability if the *Bacillus* thuringiensis Cry4B Toxin

In Protein Network Symposium on Protein Structure and Molecular Enzymology August 29-30, 2002, Faculty of Science, Mahidol University

3.3 Characterization of Protein Unfolding for *Bacillus thuringiensis* Cry4B Toxin by Stopped-f low Circular Dichroism Spectroscopy

In Protein Network Symposium on Protein Structure and Molecular Enzymology August 29-30, 2002, Faculty of Science, Mahidol University

3.4 Basic Structure of the insecticidal protein from Bacillus thuringiensis
In "Bacillus thuringiensis Symposium: From Basic to Applied Research"
May 22-23, 2003, Institute of Molecular Biology and Genetics, Mahidol University

3.5 Investigation of Molecular Stabilization and Charge Interaction in the Conserved Regions of *Bacillus thuringiensis* Cry4B Toxin

In The 28<sup>th</sup> Science and Technology of Thailand Congress October 24-26, 2002, Queen Sirikit Convention Center

3.6 Site-Directed Mutagenesisand Stability Characterization of Mosquitocidal Cry4B Toxin:

A Contribution of Hydrophobic Residues on Helix α5 Regions In The 28<sup>th</sup> Science and Technology of Thailand Congress October 24-26, 2002, Queen Sirikit Convention Center

## 4. Graduate student training / MSc. thesis

Miss Wanwarang Pathaichindachote
Mr Apichai Bourchookarn
Miss Anchanee Sangcharoen

# MUTATION OF THE HYDROPHOBIC RESIDUE ON HELIX α5 OF THE *BACILLUS THURINGIENSIS* CRY4B AFFECTS STRUCTURAL STABILITY.

Chartchai Krittanai\*, Apichai Bourchookarn, Wanwarang Pathaichindachote and Sakol Panyim

Laboratory of Molecular Biophysics, Institute of Molecular Biology and Genetics, Mahidol University, Salaya Campus, Phuttamonthon 4 Road, Nakhonpathom, 73170, Thailand; Email: stckt@mahidol.ac.th

Abstract: Cry4B toxin is a mosquito-larvicidal protein from the *Bacillus thuringiensis* subsp. *israelensis*. We have investigated the role of two conserved hydrophobic residues of Cry4B in structural stabilization. Substitutions of the leucine-175 and isoleucine-189 on helix  $\alpha$ 5 with valine and leucine did not affect the expression level, solubility and proteolytic processing. Steady state analysis of an unfolding experiment as monitored by circular dichroism and fluorescence spectroscopy demonstrated a typical two-state transition. The determined unfolding free energy for the L175V mutant revealed a structural destabilization of 10.49 kcal/mol relative to the wild type. However unfolding kinetic analysis gave identical activation energy for wild type and both mutants. Our findings suggested that a perturbation on the close packing of the hydrophobic side chains in protein interior could lead to a significant destabilization of the native conformation.

Keywords: Bacillus thuringiensis, protein folding, hydrophobic packing, free energy, mutagenesis, circular dichroism, intrinsic fluorescence.

## INTRODUCTION

Since a general globular protein folds in a way that keeps the hydrophobic side chains inside the interior and avoids contact with physiological water, hydrophobic interaction has been proposed to be one of the major driving forces for protein folding [1, 2]. Recently an optimal van der Waals close packing of the side-chain has been shown to also play a significant role in stabilization of the molecular structure [3, 4]. Several site-directed mutagenesis studies on the buried non-polar amino acid have reported an effect on structural folding and stability [5-8]. These mutational effects can be experimentally determined as a change of free energy in an unfolding/refolding process. A number of small or single-domain proteins such as ribonuclease [9], myoglobin [10], chymotrypsin inhibitor [11], straphylococcal nuclease [12], lysozyme [13] and barnase [14] have been energetically studied. However, a study on a larger protein like Cry4B is

still lacking. Even though the unfolding study of the proteins in the same family such as Cry1Ab, Cry1Ac and Cry3Aa [15-17] have been published. These works were somewhat qualitative and not directly involved with energetic effect of mutation.

The Cry4B toxin from *Bacillus thuringiensis* subsp. *israelensis* (Bti) is a protein with specific toxicity to *Aedes* mosquito larvae. The 130-kDa protoxin form is generally converted into a 65-kDa functional molecule by proteolytic processing inside the midgut of larvae. X-ray structure of Cry4B showed a similar fold to other Cry toxins like Cry1A and Cry3A [18-20]. Domain I, a seven-helical bundle, has been proposed to function as a membrane pore-forming domain [21]. Domain II and III were suggested to be involved in the membrane binding [22, 23]. Several works on site-directed mutagenesis have reported significant changes of the biochemical properties of the mutants, especially when the mutation was introduced on the central helix  $\alpha$ 5 [24-26]. These effects include a complete loss of solubility, mosquito-larvicidal activity, and increased sensitivity for proteolytic digestion. These abnormalities were proposed as a result of incorrect folding of the toxin structure or molecular destabilization upon perturbation on the critical amino acid residues.

This work aims to characterize the mutational effect of the hydrophobic residues, L175 and I189, on the central helix  $\alpha 5$  of domain I. These two residues were selected based on their conservation among the toxin family and they are well buried inside a hydrophobic core of the domain. The L175V and I189L mutants were constructed and their conformational states in the unfolding experiment were monitored by circular dichroism and fluorescence spectroscopy. The unfolding free energy and activation energy was experimentally determined and compared to the template toxin. The differences in energetic parameters can then reveal an energetic role of specific mutation on structural folding and molecular stability.

### MATERIALS AND METHODS

Site-directed mutagenesis: PCR based site-directed mutagenesis was performed on the pMU388/R203Q plasmid containing cry4B gene with previous point mutation for R203Q mutant. The reaction employed a pair of forward and reverse synthetic oligonucleotide primers (Genset, Singapore) under a high fidelity Pfu DNA polymerase (Promega, USA). Parental DNA template was removed by DpnI digestion. E. coli strain JM109 was transformed with mutant plasmids and screened by restriction analysis. DNA sequences were confirmed by analysis on an ABI-PRISM 377 automated sequencer (Perkin Elmer, USA).

*Protein expression and purification*: Expression was performed with 0.1 mM IPTG induction in LB broth containing a 100-μg/ml ampicillin at 37 °C for 12-16 hours. After cell disruption by French Press Cell, an inclusion product was solubilized in 50 mM carbonate buffer pH 10.0 and processed with TCPK-treated trypsin. Purified protein was obtained from Superdex-200 HR10/30 size-exclusion column (Amersham). Protein concentration was determined based on a far-UV absorption on using a Cary300 Bio UV-Visible spectrophotometer (Varian, Australia). Conc. (in mg/ml) = 0.144 x (A<sub>215</sub> – A<sub>225</sub>) [27].

Steady state unfolding: The purified protein was incubated in a series of GuHCl concentrations from 0-6.0 M overnight. The conformational state was monitored at 25 °C by circular dichroism and

fluorescence spectroscopy. Accurate concentration of GuHCl stock was determined from a refractive index measurement as described by Nozaki [28].

Unfolding kinetics: Fluorescence spectra were obtained in a rapid mixing between protein in carbonate buffer pH 10.0 and various proportions of GuHCl. The experiment was performed with a final protein concentration of  $10 \mu g/ml$ . All solutions and sample were degassed well before mixing.

Circular dichroism measurement: CD spectra were obtained from a Jasco J-715 spectropolarimeter (Jasco, Japan). Instrument was calibrated with 1.0 mg/ml of (+)-10-camphorsulphonic acid (CSA) and purged with nitrogen. Samples (0.4-0.6 mg/ml protein) were analyzed at 25°C in a cuvette with 0.02-cm path length. Scanning was set from 190 to 260 nm with 20-nm/min scanning rate, 1.0-second response time, and 50-millidegree sensitivity for at least 4 accumulations. All sample spectra were subtracted with baseline.

Intrinsic fluorescence measurement: Intrinsic emission fluorescence spectra were recorded from 300 to 500 nm on a Perkin Elmer LS-50B luminescence spectrometer. Excitation was set at 280 nm. Samples containing 20-40 µg/ml of protein were analyzed in a cuvette with 0.5-cm path length. Scanning rate was controlled at 50 nm/min. At least three repetitive scans were recorded and averaged.

Data Analysis: The unfolding curves were derived from changes of CD intensity at 222 nm and the fluorescence emission ratio 340/350 nm ( $F_{340/350}$ ). Apparent fraction of unfolding ( $f_{app}$ ) was calculated from an equation:

$$f_{\text{app}} = I_{\text{obs}} - (\alpha_{\text{N}} + \beta_{\text{N}} [\text{C}])$$
$$(\alpha_{\text{U}} + \beta_{\text{U}} [\text{C}]) - (\alpha_{\text{N}} + \beta_{\text{N}} [\text{C}])$$

Where  $I_{\text{obs}}$  is an observed spectral intensity,  $\alpha_{\text{N}}$  and  $\alpha_{\text{U}}$  are Y-intercept for native and unfolded state.  $\beta_{\text{N}}$  and  $\beta_{\text{U}}$  are slopes at low and high GuHCl concentration. [C] is the GuHCl concentration. Transitional midpoint, [C]<sup>50%</sup> and unfolding free energy of protein in an absence of denaturant,  $\Delta G^{\circ}_{(\text{H2O})} = m[\text{C}]^{50\%}$  at 25 °C were determined by fitting with the model equation [29]:

$$f_{\text{app}} = \frac{(\alpha_{\text{N}} + \beta_{\text{N}} [\text{C}]) + (\alpha_{\text{U}} + \beta_{\text{U}} [\text{C}]) \exp^{|m|(|\text{C}| - |\text{C}|} 50\%)|/\text{RT}}{1 + \exp^{|m|(|\text{C}| - |\text{C}|} 50\%)|/\text{RT}}$$

For kinetic data, the exponential decay were fitted to the first order kinetic using the equation:

$$I_t = I_{\alpha} + \Delta I exp^{-kt}$$

Where  $I_t$  and  $I_\alpha$  is an observed intensity and intensity at the infinite.  $\Delta I$  is the maximum intensity change. Rate constant from the fitting was then used to calculate for the free energy of activation (Ea).

$$K = (k_{\rm B}T/h)\exp^{(-Ea/RT)}$$

When  $k_B$  and h is the Boltzmann's and Plank's constants. T and R is an absolute temperature and molar gas constant. The reported free energy of activation in an absence of denaturant  $Ea^{\circ}_{(H2O)}$  was obtained from a linear plot of Ea and GuHCl concentration.

### RESULTS AND DISCUSSION

### Construction and biochemical characterization of mutants

There are a number of works that showed an anomaly from site-directed mutagenesis studies of several Cry toxins, especially when a substitution was made on the amino acid residues located on the

central helix region of domain I [24-26]. Those mutants were found to be highly susceptible to the proteolytic digestion, with complete loss of toxin solubility and mosquito-larvicidal activity. According to the recently elucidated three-dimensional structure of the 65-kDa active toxin, the two investigated hydrophobic residues L-175 and I-189 in this work are located on the central helix  $\alpha 5$  [18]. Any substitutions made at these two positions are expected to bring a directed perturbation into the domain interior. Interestingly, our constructed mutants, L175V and I189L have demonstrated native-like properties. They had a similar expression level, solubility in alkali buffer, and resistance to the proteolytic digestion (data not shown). It is appeared that the perturbation introduced by our side chain substitutions was too gentle to disrupt the general folding of the toxin. However this gave us an excellent opportunity to prepare these samples in a solution and then characterize them further for structural stability.

#### Steady-state unfolding analysis

Steady state unfolding has displayed a conformational change from the native to unfolded state upon an increasing concentration of GuHCl. Circular dichroism spectra representing the protein in native state were comprised of two negative bands around 208 and 222 nm and one intense positive band around 192 nm (Figure 1a). A significant loss of secondary structure was observed when the protein was incubated with an increasing concentration of denaturant. This unfolded state was represented by the CD spectra containing a single negative band with decreased intensity. The unfolding curves derived from the maximal change of CD intensity at 222 nm demonstrated a sigmoidal shape. The experiment was also performed in parallel by using intrinsic emission fluorescence. The transition from native to unfolded state was observed as an intensity change and a shift of  $\lambda$ max from 340 to 350 nm (Figure 1b). It was found that the unfolding

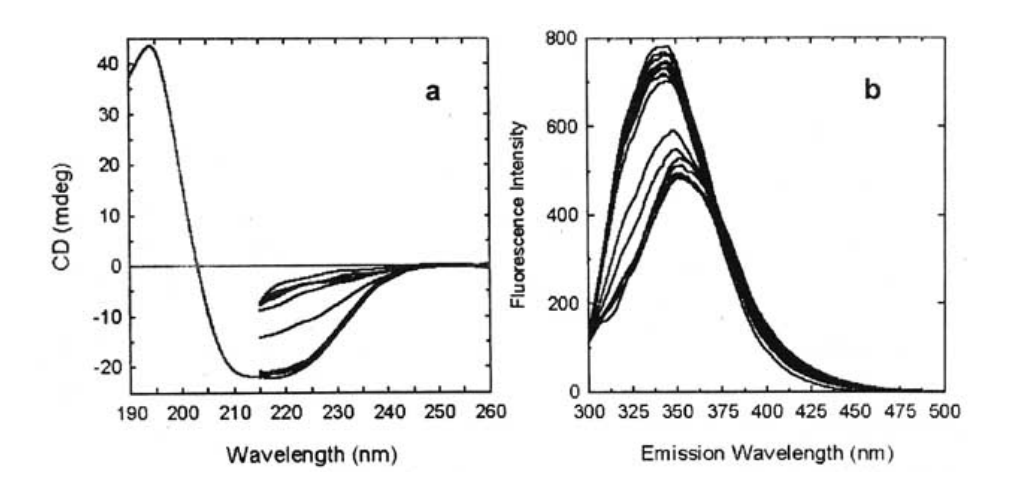
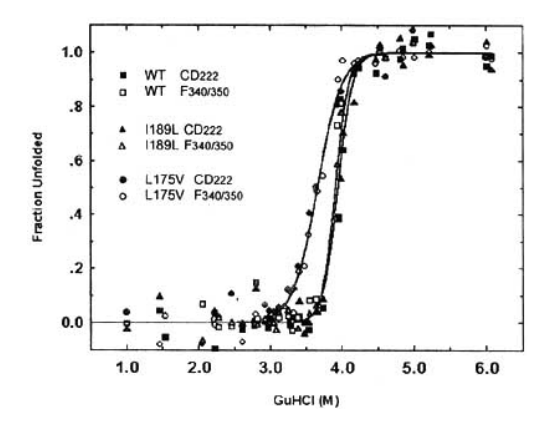


Figure 1. Conformational changes of toxins from native to unfolded states as monitored by (a) circular dichroism and (b) fluorescence spectroscopy.

curves derived from both CD and fluorescence spectra were identical. The obtained sigmoidal curves for both wild type and mutants are basically assumed as an indication for the two-state transition (Figure 2). These transitions were rapid and there was apparently no sign of stable intermediate detected. Since an analysis for unfolding free energy by extrapolation of the calculated free energy to the denaturant-free condition is sometimes not reliable [29], our free energy determination was performed based on the fitting model. The calculated unfolding free energies in an absence of denaturant ( $\Delta G^{o}_{H2O}$ ) for wild type, I189L and L175V were 23.10, 22.78 and 12.61 kcal/mol respectively. In general these free energies represent an energy gap between the native and unfolded state of proteins. Based on the baseline value obtained from the wild type, the mutation of isoleucine to leucine at position 189 seems to have no effect on structural stability of the protein. On the other hand, the mutation of leucine to valine at position 175 has a significant effect on the free energy. It was obvious that the perturbation introduced by this mutation can narrow down the energy gap and destabilize the native state up to 10.49 kcal/mol. Since the mutation from leucine to valine should not change any charge interaction, side-chain polarity or hydrogen bond, the explanation for the destabilization is likely to be an effect from the perturbation of van der Waals close packing of the hydrophobic side-chains. This suggesting justification is in good agreement with several studies in which protein stability were modulated by an improper closed-packing of the hydrophobic side-chains, especially when the perturbation was introduced inside structural interior [3-5].



**Figure 2.** Unfolding curves of Cry4B and its mutants. The unfolding free energy determined from these curves were 23.10, 22.78 and 12.61 kcal/mol for wild type, I189L and L175V respectively.

## Unfolding kinetics analysis

Apart from the steady state analysis in which the only initial and final states are taken into account, we have extended our investigation to determine whether the introduced perturbation affects the unfolding transition. In the kinetic experiment, fluorescence intensity corresponding to the native state at 340 nm was found to decrease rapidly upon a mixing of purified protein with GuHCl. An exponential decay

trace can be interpreted as an indication for a fast transition from native to unfolded state (**Figure 3a**). Rate constants from the best fit to the first order kinetics revealed a linear dependence between their logarithms and denaturant concentration (**Figure 3b**). The calculated activation energy in an absence of denaturant for wild type, L175V and I189L were 25.88, 25.75 and 25.54 kcal/mol respectively. Since these obtained values were virtually the same, we can assume that the mutations in both mutants do not affect the energy barrier or the mechanism of the unfolding transition.

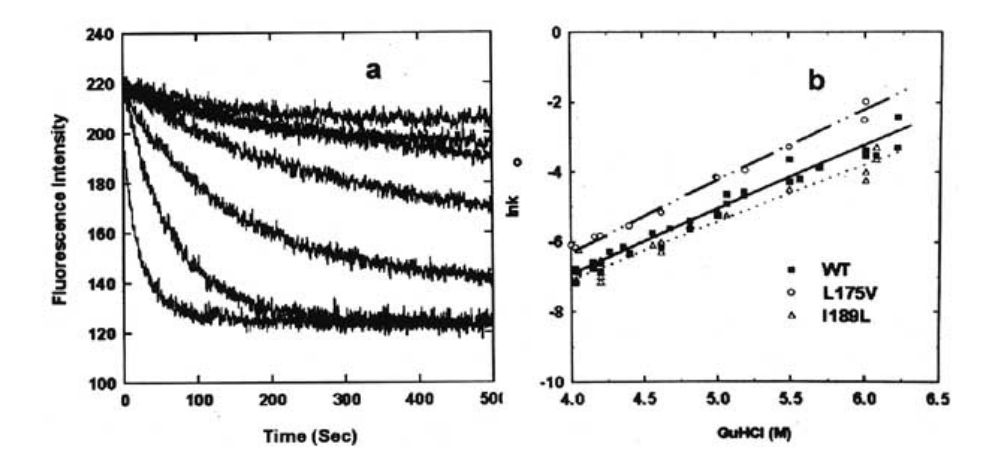


**Figure 3.** (a) Exponential decay of the fluorescence intensity at 340 nm after the protein was mixed with various GuHCl concentrations. (b) The linear plot of lnk against GuHCl concentrations. An activation energy (Ea) derived from these plots were 25.88, 25.75 and 25.54 kcal/mol for wild type, L175V and I189L respectively.

### Reaction coordinates and mutational effect

To maintain structural and functional significance, most proteins are stabilized in the native state with conformational energy around 5-20 kcal/mol lower than the unfolded state [30]. The conformational free energy of the template proteinin this work (ca. 23 kcal/mol) was comparable to those reported values. The positive sign of the calculated free energy also indicates that the transition from folded to unfolded state is spontaneous. The graphical view of unfolding can be illustrated as a path from the native state at lower energy to the unfolded state at higher energy. The determined free energy and activation energy obtained from our steady state and kinetic analysis were combined to describe the unfolding coordinates of Cry4B (Figure 4). This reaction coordinate has provides us a quantitative means to reveal a mutational effect of specific residue on structural folding and stability of the toxin. In this work the mutational effect on unfolding free energy of L175V were much larger than I189L mutant (ca.10.49 kcal/mol). An analysis on rotamer optimization in both mutants suggested that the destabilization effect in L175V is probably due to a marked loss of van der Waals contact while it remains unchanged in I189L mutant (data not shown). This similar interior cavity has also been reported to affect structural stabilization in other proteins including

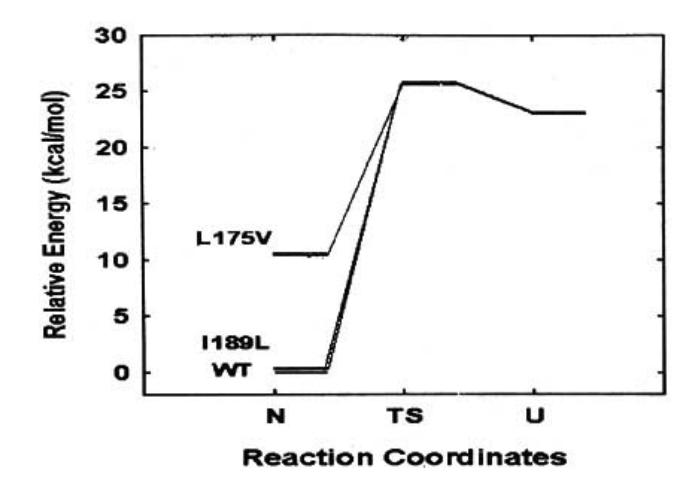


**Figure 4.** A graphical view of reaction coordinate for an unfolding of wild type and mutant Cry4B constructed from the steady state free energy and kinetic activation energy.

staphylococcal nuclease [3]. However activation energy for the unfolding of these two mutants were maintained to the same value of their template (ca.25.54-25.88 kcal/mol). It was apparent that the introduced mutation has a significant effect only on the stabilization of folded state without participating in the unfolding mechanism of the toxin.

## **ACKNOWLEDGEMENTS**

This work was supported by the Thailand Research Fund (TRF).

### REFERENCES

- [1] Dill, K.A. (1990) Biochemistry; 29, 7133-55.
- [2] Li, H., Tang, C. and Wingreen, N.S. (1997) Phys. Rev. Letts., 79, 765-68.
- [3] Chen, J. and Stites, W.E. (2001) Biochemistry, 40, 14004-11.
- [4] Holder, J.B., Bennett, A.F., Chen, J., Spencer, D.S., Byrne, M.P. and Stites, W.E. (2001) Biochemistry, 40, 13998-14003.
- [5] Prevost, M., Wodak, S.J., Tidor, B. and Karplus, M. (1991) Proc. Natl. Acad. Sci., 88, 10880-84.
- [6] Lorch, M., Mason, J.M., Sessions, R.B. and Clarke, A.R. (2000) *Biochemistry*, 39, 3480-85.
- [7] Funahashi, J., Takano, K., Yamagata, Y. and Yutani, K. (1999) Protein Eng., 12, 841-50.
- [8] Ishikawa, K., Nakamura, H., Morikawa, K. and Kanaya, S. (1993) *Biochemistry*, 32, 6171-78.
- [9] De Vos, S., Backmann, J., Prevost, M., Steyaert, J. and Loris, R.(2001) Biochemistry, 40, 10140-49.
- [10] Gupta, R., Yadav, S., Ahmad, F. (1996) Biochemistry 35, 11925-30.
- [11] Roesler, R.K., Rao, A.G. (1999) Protein Eng., 12, 967-73.
- [12] Eftink, M.R., Ionescu, R., Ramsey, G.D. and Wong, C.Y., (1996) Biochemistry, 35, 8084-94.
- [13] Xu, J., Baase, W.A., Baldwin, E. and Matthews, B.W. (1998) Protein Sci., 7, 158-77.
- [14] Pace, C.N., Laurents, D.V., Erickson, R.E. (1992) Biochemistry, 31, 2728-34.
- [15] Choma, C.T. and Kaplan, H. (1990) Biochemistry, 29, 10971-7.
- [16] Feng, Q. and Becktel, W.J. (1994) Biochemistry, 33, 8521-6.
- [17] Potekhin, S.A., Loseva, O.I., Tiktopulo, E.I. and Dobritsa AP. (1999) Biochemistry 38, 4121-7.

- [18] Boonserm, P. (2002) Ph.D Thesis, Department of Biochemistry, University of Cambridge.
- [19] Grochulski, P., Masson, L., Borisova, S., Pusztai-Carey, M., Schwartz, J.L., Brousseau, R. and Cygler, M. (1995) J. Mol. Biol., 254, 447-64.
- [20] Li, J., Carroll, J. and Ellar, D.J. (1991) Nature, 353, 815-21.
- [21] Uawithya, P., Tuntitippawan, T., Katzenmeier, G., Panyim, S. and Angsuthanasombat, C.(1998) *Biochem. Mol. Biol. Int.*, 44, 825-32.
- [22] de Maagd, R.A., Bakker, P.L., Masson, L., Adang, M.J., Sangadala, S., Stiekema, W. and Bosch, D. (1999) *Mol. Microbiol.*, 31, 463-71.
- [23] Smith, G.P. and Ellar, D.J. (1994) Biochem. J., 302, 611-6.
- [24] Nunez-Valdez, M., Sanchez, J., Lina, L., Guereca, L. and Bravo, A. (2001) *Biochim. Biophys. Acta.* 81546, 122-31.
- [25] Lungchukiet, P. (2000) MSc. Thesis, Institute of Molecular Biology and Genetics, Mahidol University.
- [26] Pathaichindachote, W. (2002). MSc. Thesis, Institute of Molecular Biology and Genetics, Mahidol University.
- [27] Waddell, W.J. (1956) J. Lab. Clin. Med., 48, 311-14.
- [28] Nozaki, Y. (1972) Methods Enzymol., 26, 43-50.
- [29] Ibarra-Molero, B., Sanchez-Ruiz, J.M. (1996) Biochemistry, 35, 14689-702.
- [30] Gromiha, M.M., An, J., Kono, H., Oobatake, M., Uedaira, H. and Sarai, A. (1999) Nucleic Acids Res., 27, 286-288.

Received on March 3, 2003, accepted on April 28, 2003.